Physiological and Proteomic Analysis of Salinity Tolerance in *Puccinellia tenuiflora*

Juanjuan Yu,[†] Sixue Chen,[‡] Qi Zhao,[†] Tai Wang,[⊥] Chuanping Yang,[†] Carolyn Diaz,[‡] Guorong Sun,*[,ǁ] and Shaojun Dai*[,†,§]

[†]Alkali Soil Natural Environmental Science Center, Northeast Forestry University,
 Key Laboratory of Saline-alkali Vegetation Ecology Restoration in Oil Field, Ministry of Education, Harbin 150040, China

[‡]Department of Biology, Genetics Institute, Interdisciplinary Center for Biotechnology Research, University of Florida,
 Gainesville, Florida 32610, United States

[§]College of Life Science and Technology, Harbin Normal University, Harbin 150080, China

[ǁ]Binzhou Polytechnic College, Binzhou, Shandong 256603, China

[⊥]Institute of Botany, Chinese Academy of Sciences, Beijing 100093, China

Ⓢ Supporting Information

ABSTRACT: Soil salinity poses a serious threat to agriculture productivity throughout the world. Studying mechanisms of salinity tolerance in halophytic plants will provide valuable information for engineering plants for enhanced salt tolerance. Monocotyledonous *Puccinellia tenuiflora* is a halophytic species that widely distributed in the saline-alkali soil of the Songnen plain in northeastern China. Here we investigate the molecular mechanisms underlying moderate salt tolerance of *P. tenuiflora* using a combined physiological and proteomic approach. The changes in biomass, inorganic ion content, osmolytes, photosynthesis, defense-related enzyme activities, and metabolites in the course of salt treatment were analyzed in the leaves. Comparative proteomic analysis revealed 107 identities (representing 93 unique proteins) differentially expressed in *P. tenuiflora* leaves under saline conditions. These proteins were mainly involved in photosynthesis, stress and defense, carbohydrate and energy metabolism, protein metabolism, signaling, membrane, and transport. Our results showed that reduction of photosynthesis under salt treatment was attributed to the down-regulation of the light-harvesting complex (LHC) and Calvin cycle enzymes. Selective uptake of inorganic ions, high K^+/Na^+ ratio, Ca^{2+} concentration changes, and an accumulation of osmolytes contributed to ion balance and osmotic adjustment in leaf cells. Importantly, *P. tenuiflora* plants developed diverse reactive oxygen species (ROS) scavenging mechanisms in their leaves to cope with moderate salinity, including enhancement of the photorespiration pathway and thermal dissipation, synthesis of the low-molecular-weight antioxidant α-tocopherol, and an accumulation of compatible solutes. This study provides important information toward improving salt tolerance of cereals.

KEYWORDS: proteomics, halophyte, *Puccinellia tenuiflora*, salinity tolerance

■ INTRODUCTION

Soil salinity is one of the most significant limiting factors that affect the distribution and productivity of major crops worldwide.[1−3] More than 6% of the world's land is affected by salt,[1] and increased salinization may lead to the loss of 30% arable land in the next 25 years and up to 50% by 2050.[4] This severe situation has stimulated interest in plant engineering for salt tolerance.[1−3] Studies of salt tolerance mechanisms in plants will provide valuable information for effective engineering strategies.

Some studies have been carried out on both glycophytes and halophytes to reveal the physiological and molecular changes in response to salt stress.[1−3] Compared with glycophytes, halophytes have developed unique structures to tolerate salt stress, including salt glands, bladder hairs, succulent tissues, thick layers of suberin, and double layers of suberized cells in the roots.[5,6] In addition, halophytes have evolved more salt-responsive genes than glycophytes. These genes have made halophytes highly efficient in selective ion accumulation/exclusion, control of ion uptake/transport, compartmentalization of ions, synthesis of compatible products, change in photosynthetic and energy metabolism, induction of antioxidative enzymes and hormones, and modification of cell membrane/wall structure.[2,3] Some of the salt-responsive genes have been cloned from halophytes and then transferred to glycophytes for improving salt tolerance.[6] Examples are *NHX1* (a tonoplast Na^+/H^+ antiporter encoding gene),[6]

BADH (a betaine aldehyde dehydrogenase encoding gene),[7,8] *DREB1* (an EREBP/AP2-type DNA binding protein encoding gene),[9] and *MIPS* (a gene encoding L-myo-inositol-1-phosphate synthase).[10]

Although certain genes play important roles, it is the network of multiple signaling and metabolic pathways that mediate plant salt response/tolerance. To further understand salt-tolerance networks, transcriptional analyses have been carried out in some halophytes under salt stress, including *Thellungiella halophila*,[11−14] *Suaeda salsa*,[15] *Aeluropus littoralis*,[16] *Salicornia brachiata*,[17] and *Festuca rubra* ssp. *litoralis*.[18] More than 2,300 ESTs/cDNAs have been identified to exhibit differential expression in the aforementioned halophytes under salt stress. Most of the genes encode signaling molecules, transporters, transcriptional regulators, membrane fluidity-related proteins, photosynthesis proteins, and stress-related enzymes (e.g., those involved in osmolyte biosynthesis, reactive oxygen species (ROS) scavenging, and ion homeostasis). Recently, high-throughput comparative proteomics approaches have been used to investigate the mechanisms of salt tolerance in halophytes.[19−25] More than 218 salt-responsive proteins were identified in dicotyledonous halophytes, such as *Salicornia europaea*,[19] *Suaeda aegyptiaca*,[20] *Bruguiera gymnorhiza*,[21] *T. halophila*,[22] and *Aster tripolium*.[25] The dynamic protein expression patterns in these plants revealed that photosynthesis, energy metabolism, ROS scavenging, and ion homeostasis played important roles in salt tolerance.[19−22] However, few proteomic investigations in monocotyledonous halophytes have been reported.[23,24] Sobhanian et al.[23] investigated a C4 monocotyledonous halophyte *Aeluropus lagopoides*. Their results showed that the plants exhibited enhanced energy production, amino acid biosynthesis, C4 photosynthetic pathway, and detoxification under salinity conditions. In addition, wild halophytic rice (*Porteresia coarctata*), a species of C3 monocotyledonous halophytes, employs the following strategies to deal with salinity: enhanced production of energy and osmotic compounds, alteration of transcriptional activity and protein modification, and change in cell wall components.[24] Further systematic characterization of the salt-tolerance characteristics in monocotyledonous halophytes will aid rational engineering of cereal crops for enhanced salt tolerance.

Puccinellia tenuiflora is a monocotyledonous halophyte species belonging to the Gramineae and has outstanding nutritional value for livestocks. It can thrive in the saline-alkali soil of the Songnen plain in northeastern China. Some physiological mechanisms of *P. tenuiflora* in response to salt/alkali treatments have been previously studied. *P. tenuiflora* can accumulate inorganic ions, proline, betaine, and organic acid for osmotic adjustment.[26−28] The plants have evolved stronger selectivity for K^+ over Na^+ to maintain a high cytoplasmic K^+/Na^+ ratio, while leaf ion secretion contributes little to ion balance.[29−31] In addition, some antioxidant enzymes involved in ROS scavenging were found to be enhanced.[32] Furthermore, some ion-responsive antiporter/channel genes have been studied: (1) *PutPMP3-1* and *PutPMP3-2* encoding plasma membrane protein 3 family proteins function to prevent the accumulation of excess Na^+ and K^+ ions;[33] (2) *PutHKT2;1* encoding a high-affinity K^+ transporter plays a role in K^+ uptake to maintain a high ratio of K^+/Na^+ in the cells;[34] (3) *PutAKT1* encodes a plasma membrane-localized K^+ channel family protein that can interact with KPutB1 to alter K^+ and Na^+ homeostasis;[35,36] (4) *PutCAX1* encoding a Ca^{2+}/H^+ antiporter in the vacuolar membrane was proposed to play a role in Ca^{2+}, Ba^{2+}, and Zn^{2+} transport;[37] and (5) *PtNHA1* encodes a

Na^+/H^+ antiporter for the maintenance of low cytosolic Na^+.[38] Despite this progress, the precise molecular mechanisms in *P. tenuiflora* to cope with salinity need to be investigated further.[30,39]

Plant salt tolerance is controlled by complex and sophisticated molecular networks. It displays common as well as specific characteristics in different species of halophytes. Here we report the study of the salt-responsive characteristics of halophyte *P. tenuiflora* under 0, 50, and 150 mM NaCl conditions for 7 days using physiological and comparative proteomic approaches. We found unique mechanisms of osmotic adjustment, ion balance, photosynthesis, antioxidation, and secondary metabolism underlying salt tolerance in *P. tenuiflora*. Our results lay a solid foundation necessary for further investigation of the salt tolerance networks.

■ EXPERIMENTAL PROCEDURES

Plant Material, Treatment, and Biomass Analysis

Seeds of *Puccinellia tenuiflora* (Turcz.) scribn. et Merr. were sowed on pearlite and grown in Hoagland solution in a controlled environment chamber under fluorescent light (300 μmol m^{-2} s^{-1}; 13 h light/11 h dark) at 25 °C and 75% humidity for 50 days.[32] Seedlings of 50-day old were treated with 0, 50, and 150 mM NaCl, respectively, for 7 days. To maintain a stable NaCl concentration in the Hoagland medium, culturing solutions were changed daily, and the ion content and osmotic potential in solution were monitored using a SevenMulti Neutral meter (Mettler Toledo, U.K.) with ion-selective electrode and a vapor pressure osmometer (Wescor 5520, USA), respectively. After 7 days of treatment, leaves were harvested and either used fresh or immediately frozen in liquid nitrogen and stored at −80 °C for physiological and proteomic experiments. At least three independent biological replicates for each treatment were conducted for all the experiments. Shoot length and fresh weight (FW) were measured right after harvesting. Dry weight (DW) was determined after dehydration at 60 °C until to a constant weight. Leaf water content was estimated as the difference between fresh weight and dry weight divided by the fresh weight.

Leaf Micro- and Ultrastructure Analysis and Chloroplast Protein Extraction

Leaf micro- and ultrastructure were analyzed according to the method of Cao et al.[40] Images were taken using a microscope (Axioskop 40 Fluorescence Microscope, Zeiss, Germany) and a transmission electron microscope (JEOL-2000, USA). Intact chloroplasts were isolated according to the method of Ni et al.[41] Protein was extracted using a phenol method.[42]

Total Soluble Sugar, Proline, and Osmotic Potential Analysis

Proline content and total sugar levels were determined using ninhydrin reaction and an anthrone reagent as previously described.[43] Osmotic potential was determined in pressed sap of leaves using a vapor pressure osmometer (Wescor 5520, USA).

Ion Content Analysis

The relative content of K and Na on the leaf surface was analyzed using a XL-30 surrounding scanning electron microscope (The Netherlands Phillips Company, Netherland) and a Kevex energy peatrometer (American Thermo Company, USA) according to the method of Sun et al.[31] The content of K^+, Na^+, Ca^{2+}, and Mg^{2+} in the leaves was determined using an atomic absorption spectrophotometer (PerkinElmer AAnalyst 800, USA) after drying the leaves in a 80 °C oven until a constant weight was

reached. The Cl^- content was determined using a spectrophotometer (UltrospecTM 2100 pro UV/Visible, GE Healthcare), with acetone as colloid protecting agent. The content of PO_4^{3-}, NO_3^-, and NH_4^+ was determined by phosphorus molybdenum blue spectrophotometric method, salicylic acid/concentrated sulphuric acid method, and phenol/hypochlorite reaction, respectively.

Photosynthesis and Chlorophyll Fluorescence Analysis

Net photosynthetic rate (Pn), stomatal conductance (Gs), intercellular CO_2 (Ci), and transpiration rate (Tr) were determined at 10:00 a.m. using a portable photosynthesis system LI-COR 6400 (LI-COR Inc., USA). Water usage efficiency (WUE) was calculated from Pn divided by Tr. Dissolved oxygen (DO) was detected by dissolved oxygen probes, and then the relative tissue CO_2 and O_2 levels were evaluated by the percentage of Ci and DO of each NaCl condition (50 and 150 mM NaCl) over that of the normal condition (0 mM NaCl). The chlorophyll fluorescence parameters were recorded by using a pulse-amplitude-modulated (PAM) chlorophyll fluorometer (Dual-PAM-100) (Walz, Effeltrich, Germany) and an emitter-detector-cuvette assembly with a unit 101ED (ED-101US).[44]

Enzyme Activity Assay

For superoxide dismutase (SOD), catalase (CAT), and peroxidase (POD) sample preparation, 1 g of leaf tissue was homogenized on ice in 5 mL of buffer I (50 mM phosphate buffer (pH 7.8), 0.1 mM ethylenediaminetetraacetic acid (EDTA), 4% polyvinypolypyrrolidone (PVPP), and 0.3% Triton X-100). For glutathione S-transferase (GST), pyruvate orthophosphate dikinase (PPDK), and glycolate oxidase (GO), 0.5 g of leaf tissue was ground on ice in 8 mL buffer II (50 mM Tris-HCl buffer (pH 7.5), 10 mM $MgCl_2$, 5 mM DTT, and 2% PVPP). For ascorbate peroxidase (APX) and glutathione reductase (GR), 1 g of leaf tissue was ground to a fine powder in liquid nitrogen. For the APX assay, the powder was resuspended in 50 mM phosphate buffer (pH 7.0). For the GR assay, buffer III (50 mM Tris-HCl buffer, pH 7.0, 20% glycerol, 1 mM EDTA-Na_2, 5 mM $MgSO_4$, 1 mM DTT, 1 mM glutathione (GSH), and 1 mM ascorbic acid) was used. After centrifugation at $15,000 \times g$, 4 °C for 20 min, the supernatants were used for enzyme activity assays. The activity of SOD was assayed by inhibiting the photochemical reduction of nitroblue tetrazolium (NBT) at 560 nm. One unit of SOD activity was defined as the amount of enzyme that inhibited 50% of NBT photoreduction. The activities of CAT and POD were determined by measuring H_2O_2 consumption at 240 nm and by a guaiacol method at 470 nm, respectively. One unit of CAT and POD activities were defined as the change in absorbance per minute per milligram protein and 0.01 units per minute per milligram protein, respectively. The activities of APX, GR, and GST were measured by monitoring the rate of ascorbate oxidation at 290 nm ($\varepsilon = 2.8$ mM^{-1} cm^{-1}), the absorbance change at 340 nm due to oxidation of NADPH ($\varepsilon = 6.22$ mM^{-1} cm^{-1}), and the product of CDNB conjugated with GSH absorbed at 340 nm ($\varepsilon = 9.6$ mM^{-1} cm^{-1}), respectively. Their activities were subsequently expressed as the amount of ascorbic acid oxidized, NADPH oxidized, and product of S-conjugate per minute per milligram protein, respectively. In addition, the activities of PPDK and GO were assayed by monitoring NADH utilization at 340 nm (NADH oxidation through the PEPC/MDH coupled reactions) ($\varepsilon = 6.22$ mM^{-1} cm^{-1}), and formation of glycoxylate phenylhydrazone at 324 nm ($\varepsilon = 17$ mM^{-1} cm^{-1}), respectively. Their activities were expressed as

the amount of NADH oxidized, and the products of glycoxylate phenylhydrazone per minute per milligram protein, respectively.

Analysis of Malondialdehyde (MDA) and α-Tocopherol Contents

The MDA contents were determined using previous methods.[32,43] The α-tocopherol contents were assayed according to the method of Ching and Mohamed.[46] After saponification of the samples with KOH in the presence of ascorbic acid, α-tocopherol was extracted to petroleum ether. The organic phase was removed and the solvent evaporated under a stream of nitrogen gas. α-Tocopherol was dissolved in 1 mL of methanol and quantified by HPLC (Waters 2996 Alliance, USA) using α-tocopherol (AppliChem, Germany) as standard.

Protein Sample Preparation, 2DE, and Image Analysis

Total leaf protein of seedlings under different treatments (0, 50, and 150 mM NaCl) was extracted according to the method of Wang et al.[42] Protein samples were prepared independently from three different batches of plants. Protein concentration was determined using a Quant-kit according to manufacture's instructions (GE Healthcare, USA). The protein samples were separated and visualized using 2DE approaches according to Dai et al.[47] Nine gels were run for each treatment, including three biological replicates for each sample and three technical replicates for each biological replicate. Gel image acquisition and analysis were conducted as previously described.[42] For quantitative analysis, The average vol % values were calculated from three technical replicates to represent the final vol % values of each biological replicate. Comparisons and statistical analysis were performed using the calculated average values of each biological replicate among the three different treatments. Spots with more than a 1.5-fold change among the treatments and a p value smaller than 0.05 were considered to be differentially expressed spots.

Protein Identification Using Electrospray Quadrupole Time-of-Flight (ESI-Q-TOF) Mass Spectrometry (MS) and Database Searching

The differentially expressed spots were excised from the gels and digested with trypsin.[47] MS and MS/MS spectra were acquired on a ESI-Q-TOF MS (QSTAR XL) as previously described.[48] The MS/MS spectra were searched against the NCBInr protein databases (http://www.ncbi.nlm.nih.gov/) (701,710 sequences entries in NCBI in July 25, 2009) using Mascot software (Matrix Sciences, U.K.). The taxonomic category was green plants. The searching criteria include mass accuracy of 0.3 Da, one missed cleavage allowed, carbamidomethylation of cysteine as a fixed modification, and oxidation of methionine as a variable modification. To obtain high confident identification, proteins had to meet the following criteria: (1) the top hits on the database searching report, (2) a probability-based MOWSE score greater than 43 ($p < 0.01$), and (3) more than two peptides matched with nearly complete y-ion series and complementary b-ion series present. *De novo* sequencing was conducted using PEAK 5.1 software (Bioinformatics Solutions Inc., Canada), and the results were manually inspected.

Protein Classification and Hierarchical Cluster Analysis

Protein motifs were obtained by blasting against the NCBI and UniProt database (http://www.ebi.uniprot.org/). Combined with knowledge from literature, proteins were classified into different categories. Self-organizing tree algorithm hierarchical clustering of the expression profiles was performed on the log

transformed fold change values of protein spots (http://rana.lbl.gov/EisenSoftware).[19]

Western Blot Analysis

Western blotting was conducted according to Dai et al.[47] The primary antibodies were raised in rabbits against maize pyruvate orthophosphate dikinase (PPDK), rice ribulose-1,5-bisphosphate carboxylase large unit (RuBisCO LSU), rice phosphoribulokinase (PRK), rice sedoheptulose-1,7-bisphosphatase (SBPase), and a PsbA/D1 N terminal peptide. For PPDK immunodetection, a total of 100 μg of protein from *P. tenuiflora* leaves, 150 μg of protein from *P. tenuiflora* chloroplasts, and 6 μg of protein from maize leaves were subjected to 10% SDS-PAGE, respectively. For RuBisCO LSU, PRK, SBPase, and D1 protein immunodetection, 5, 2, 30, and 10 μg of proteins from *P. tenuiflora* leaves were loaded on SDS-PAGE gels, respectively. After electroblotting, nitrocellulase membranes were blocked with 5% skimmed milk, probed with different antibodies (PPDK at 1:5000, RuBisCO LSU at 1:8000, PRK and SBPase at 1:1000, and D1 at 1:10000) for 1 h followed by three washes (10 min) using Tris buffered saline with Tween (TBST, and then incubated with horseradish peroxidase-coupled goat antirabbit antibody for 1 h followed by three washes (10 min) using TBST. Enhanced chemiluminescene was used to detect the signal. Relative abundance was analyzed using Image Master 2D Platinum Software (Version 5.0, GE Healthcare, USA).

Statistical Analysis

All results are presented as means ± standard error (SE) of at least three replicates. Data were analyzed by one-way ANOVA using the statistical software SPSS 17.0 (SPSS Inc., Chicago, USA). The treatment mean values were compared by post hoc least significant difference (LSD) test. A p value less than 0.05 was considered statistically significant.

■ RESULTS

Effect of Salt Treatment on Seedling Growth and Leaf Micro- and Ultrastructure of *P. tenuiflora*

After 7 days of treatment under 0, 50, and 150 mM NaCl, respectively, the leaves of salt-treated seedlings did not exhibit any obvious phenotype differences. The leaf fresh weight (Figure 1A), shoot length (Figure 1B), and water content (Figure 1C) were reduced, but the dry weight (Figure 1D) did not show significant reduction with the increase of NaCl concentration. Under normal condition, the vascular bundles represent typical C3 plant characteristics without obvious Kranz anatomy (Figure 2A,B). In addition, the chloroplasts/thylakoid in mesophyll cells and in bundle sheath cells looked similar (Figure 2C,D). No obvious differences were found in vascular bundles and thylakoid structure of seedlings under NaCl treatment (data not shown).

Changes of Leaf Osmotic Potential, Osmolytes, and Ion Contents

Leaf osmotic potential showed a gradual reduction with the increase of NaCl concentration (Figure 3A). In response to salt treatment, plants accumulated osmolytes for osmotic adjustment. The contents of proline, soluble sugar, and betaine in *P. tenuiflora* leaves increased dramatically under 150 mM NaCl (Figure 3B−D). Na$^+$ concentration in leaves increased sharply by 2.92 times and 16.34 times under 50 mM and 150 mM NaCl, respectively (Figure 3E), and K$^+$ concentration slightly declined under 150 mM NaCl (Figure 3F). The K$^+$/Na$^+$ ratios also decreased with increasing salt concentrations (Figure 3G).
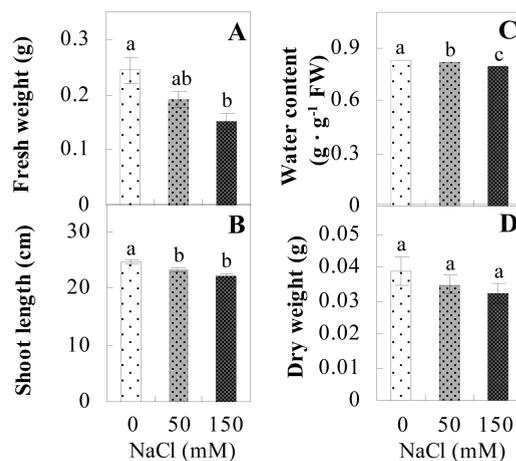

Figure 1. Biomass of *P. tenuiflora* seedlings grown under NaCl conditions. (A) fresh weight of leaves; (B) shoot length of seedlings; (C) water content in leaves; (D) dry weight of leaves. The values were determined after plants were treated with 0, 50, and 150 mM NaCl for 7 days and are presented as means ± SE (n = 50). The different small letters indicate significant (p < 0.05) difference in different treatments.
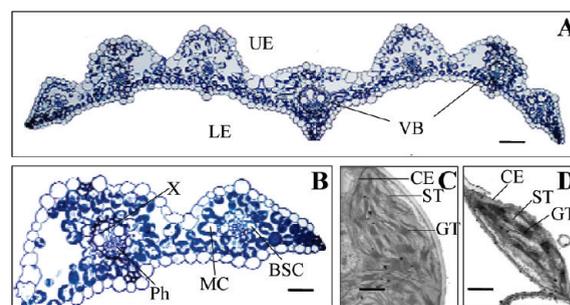

Figure 2. Micro- and ultrastructure of *P. tenuiflora* leaves under normal condition. (A) Cross-section of leaves under optical microscope, bar = 40 μm. (B) Enlarged view of vascular bundle under optical microscope, bar = 20 μm. (C) Chloroplast of mesophyll cells under transmission electron microscope (TEM), bar = 0.653 μm. (D) Chloroplast of bundle sheath cell under TEM, bar = 0.625 μm. BSC, bundle sheath cell; CE, chloroplast envelope; GT, granum thylakoid; LE, lower epidermis; VB, vascular bundle; MC, mesophyll cell; Ph, phloem; ST, stroma thylakoid; UE, upper epidermis; X, xylem.

Furthermore, the levels of Na and K on the leaf surface increased (Figure 3H,I). Ca^{2+} concentration in leaves slightly decreased under 50 mM NaCl but increased with 150 mM NaCl treatment (Figure 3J). Mg^{2+} concentration did not show any obvious changes under salt conditions (Figure 3K). In addition, some anions displayed changes in concentration under salinity. Cl$^-$ accumulated in levels with increasing salt concentration (Figure 3L), and PO$_4^{3-}$ concentration also increased under 150 mM NaCl (Figure 3M). However, NO$_3^-$ concentration declined under salt treatment (Figure 3N), and NH$_4^+$ concentration increased under 50 mM NaCl but declined under 150 mM NaCl (Figure 3O).

Effect of Salt Treatment on Photosynthesis

The Gs, Ci, Pn, and Tr decreased gradually with the increase of NaCl concentration, and the WUE increased under 150 mM NaCl treatment (Figure 4A−E). The reduced rate of intercellular CO$_2$ concentration (K$_{CO_2}$) was higher than that of O$_2$ concentration (K$_{O_2}$) with the increase of salinity (Figure 4F).
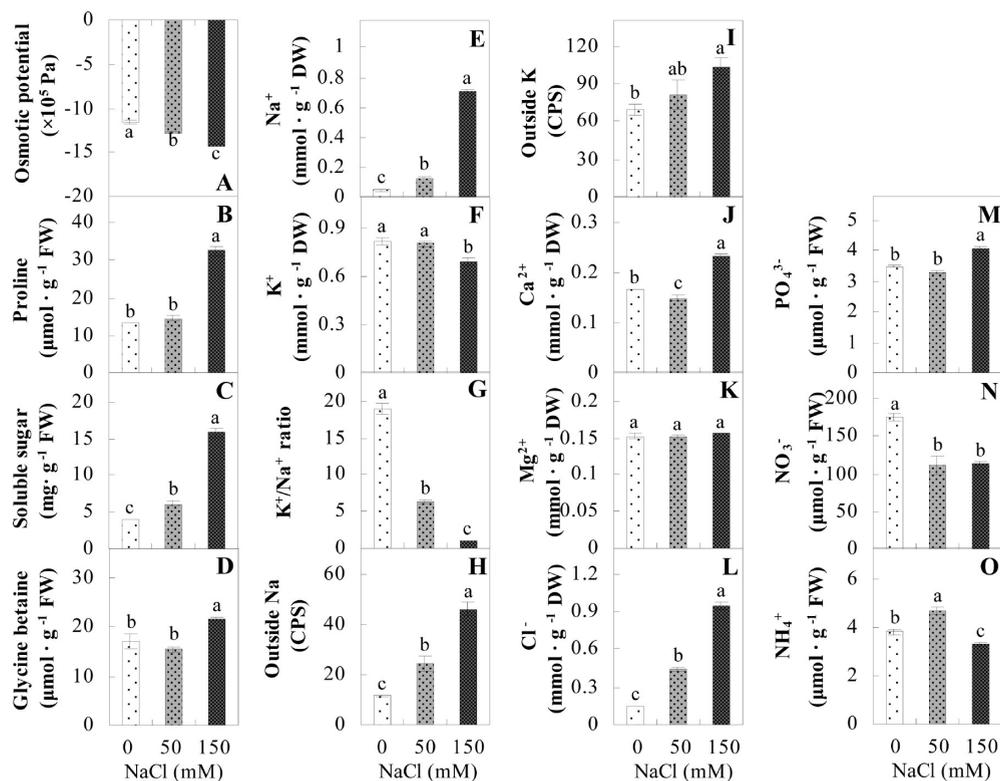
Figure 3. Effect of salinity on osmotic regulation and ionic contents in *P. tenuiflora* leaves: (A) osmotic potential; (B) proline content; (C) soluble sugar content; (D) glycine betaine content; (E) Na^+ concentration in leaves; (F) K^+ concentration in leaves; (G) K^+/Na^+ ratio in leaves; (H) relative Na content outside of the leaves; (I) relative K content outside of the leaves; (J) Ca^{2+} concentration in leaves; (K) Mg^{2+} concentration in leaves; (L) Cl^- concentration in leaves; (M) PO_4^{3-} concentration in leaves; (N) NO_3^- concentration in leaves; (O) NH_4^+ concentration in leaves. The values were determined after plants were treated with 0, 50, and 150 mM NaCl for 7 days and are presented as means $\pm$ SE ($n = 3$). The different small letters indicate significant difference ($p < 0.05$) in different treatments. CPS, counts per second.

Chlorophyll fluorescence parameters can be used to evaluate changes in photosystem II (PSII) photochemistry and linear electron flux.[49] The maximum quantum efficiency of PSII photochemistry (Fv/Fm), PSII maximum efficiency (Fv'/Fm') and fraction of PSII centers that are "open" (qL) in the leaves of salt-treated plants declined (Figure 4G−I). In addition, the actual PSII efficiency (φPSII) and electron transport rate (ETR) calculated from φPSII also decreased gradually with the increase of salt (Figure 4J,K). Nonphotochemical quenching (NPQ) increased gradually with the increase of salt concentration (Figure 4L).

Antioxidant Enzymes Activities, α-Tocopherol Content, and Plasma Membrane Integrity

Under salt conditions, the activities of different antioxidant enzymes need to be adjusted. The activities of SOD were initially increased at 50 mM NaCl and then decreased dramatically at 150 mM NaCl (Figure 5A). The activities of POD decreased slightly at 50 mM NaCl and then increased at 150 mM NaCl (Figure 5B), but the results were not significantly different from the control condition (0 mM NaCl). The activities of APX, GR, and GST did not display any significant changes under salt conditions (Figure 5C−E). In contrast, the CAT activities increased as the salt concentration increased (Figure 5F). In addition, the activities of two other salt response enzymes, PPDK and GO, showed significant increases under salt conditions (Figure 5G,H). Interestingly, an increase in the content of the nonenzyme antioxidant α-tocopherol was detected with increasing

salinity levels (Figure 5I). However, plasma membrane integrity as evaluated by MDA contents was not significantly different between control and salt-treated seedlings (Figure 5J).

Identification of Differentially Expressed Proteins under Salt Treatment

On each of the 2D gels, approximately 1,300 Coomassie Brilliant Blue-stained protein spots were detected (Figure 6). Image analysis revealed 657 common reproducible protein spots across all the samples. While the global pattern of proteins largely remained unaltered, 188 protein spots (approximately 15% of the total protein spots) were detected as differentially expressed spots ($p < 0.05$). All of the 188 differentially expressed spots were subjected to in-gel digestion and submitted for protein identification. A total of 119 protein spots were identified using ESI-Q-TOF MS and Mascot database searching (Table 1, Supporting Information Tables S1, and S2). Among them, only 93 contained a single protein each (Table 1). The remaining 26 each contained more than one protein (Supporting Information Table S2). In this case, it is difficult to determine which protein changed in abundance. Therefore, we focused on the 93 protein identities (IDs) representing 79 unique proteins (Table 1, Supporting Information Table S1). Furthermore, the MS/MS spectra acquired from the remaining 69 spots not identified by database searching were submitted for *de novo* sequencing. A total of 29 MS/MS spectra were successfully sequenced with b and y ion series, and they corresponded to 19 protein spots (Supporting Information Figure S1). The rest of the MS/MS spectra are of
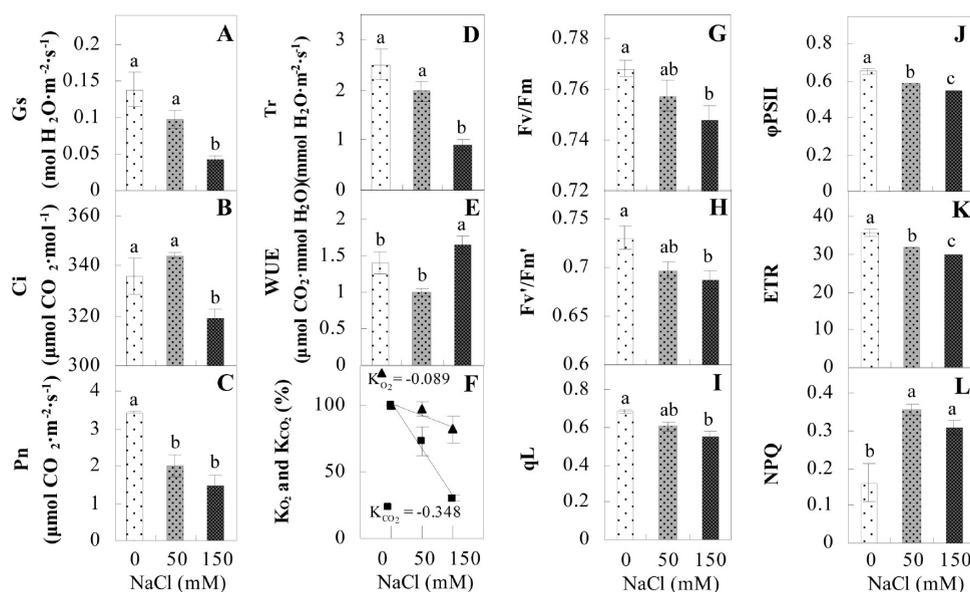
Figure 4. Photosynthetic characteristics and chlorophyll fluorescence parameters of *P. tenuiflora* leaves under salt treatment: (A) stomata conductance (Gs); (B) intercellular CO_2 (Ci); (C) photosynthesis rate (Pn); (D) transpiration rate (Tr); (E) water usage efficiency (WUE); (F) reduced rate of intercellular CO_2 concentration (K_{CO_2}) and that of O_2 concentration (K_{O_2}) with the increase of salinity; (G) Fv/Fm; (H) Fv′/Fm′; (I) qL; (J) φPSII; (K) ETR; (L) NPQ. The values were determined after plants were treated with 0, 50, and 150 mM NaCl and are presented as means ± SE (n = 3). The different small letters indicate significant difference ($p < 0.05$) in different treatments.

low quality and uninterpretable. Among the 19 protein spots, there are four proteins identified by BLAST alignments (Table 2), 10 *de novo* sequenced proteins (Table 2), and five containing a mixture of proteins (Supporting Information Table S4).

On the basis of the Gene Ontology, BLAST alignment, and information from the literature, the 107 IDs (including 93 IDs from Mascot database searching and 14 IDs from *de novo* sequencing) were classified into 11 functional categories: photosynthesis, stress and defense, carbohydrate and energy metabolism, metabolism, transcription-related, protein synthesis, protein folding and transport, protein degradation, signaling, membrane and transport, and unknown function (Tables 1 and 2; Supporting Information Figure S2A). Among the functional categories, photosynthesis (14%), stress and defense (14%), carbohydrate and energy metabolism (14%), and protein metabolism (19%) were over-represented.

To study protein expression characteristics in each functional category, hierarchical clustering analysis was performed generating two main clusters (Supporting Information Figure S2B,C). Cluster I included 80 IDs, the levels of which were decreased under salt treatment (Supporting Information Figure S2B), and cluster II contained 27 up-regulated IDs (Supporting Information Figure S2C). In addition, IDs associated with various functional categories showed a heterogeneous distribution in the two clusters. For example, most of the IDs involved in photosynthesis and stress/defense were present in cluster I, whereas carbohydrate and energy metabolism-related proteins were mainly in cluster II. These results suggest switching of biological processes occurred in the course of salt treatment.

Leaf Proteomic Characteristics under Salt Conditions

We identified 15 photosynthesis related protein IDs, including five PSII IDs, and 10 CO_2 assimilation-related IDs (Table 1). For light reaction related proteins, chlorophyll a/b binding protein (CAB) (spots 8434, 8895, and 8385) and oxygen-evolving

enhancer protein 1 (OEE 1) (spot 8251) were down-regulated under salt treatment. As to CO_2 assimilation related proteins, carbonic anhydrase (CA) (spot 8459), RuBisCO LSU (spots 8650, 8603, and 7781), ribulose-1,5-bisphosphate carboxylase small unit (RuBisCO SSU) (spot 8755), ribulose-bisphosphate carboxylase activase (spot 7789), SBPase (spot 8046), and PRK (spot 7981) were down-regulated. The photorespiratory pathway-related serine-glycine hydroxymethyltransferase (SHMT) (spot 8869) was up-regulated. To further evaluate the expressional levels of some representative photosynthetic enzymes, the abundance of RuBisCO LSU, SBPase, and PRK was confirmed to be reduced in salt-treated plants using Western blotting (Figure 7). Besides, the D1 protein, a key protein in light-harvesting complex (LHC), was also detected to be down-regulated under salt condition by immunoblot analysis (Figure 7).

Fifteen detoxification and oxidative stress-related proteins were identified. They include seven enzymatic antioxidants, one nonenzymatic antioxidant synthetic enzyme, and seven oxidative stress-related proteins. Some enzymatic antioxidants, e.g., ascorbate peroxidase (APX) (spots 8369 and 8387), peroxiredoxin-typical 2-Cys subfamily (Prx) (spots 8537 and 8279), glutathione peroxidase (GPX) (spot 8570), glutathione *S*-transferase (GST) (spot 8427), and thioredoxin-chloroplast precursor (Trx) (spot 8697), were decreased in expression under salt treatment. Several proteins, such as glyoxalase (spots 8277 and 8248), plastid lipid associated protein 3 (spot 7951), and rhodanese homology domain (spot 7503), were also reduced in NaCl-treated plants. In contrast, other antioxidant-related proteins, tocopherol cyclase (VTE1) (spot 7747) and ferredoxin-NADP(H) oxidoreductases (FNR) (spots 8084 and 9059), showed up-regulation in salt-treated plants.

We also identified 15 proteins involved in carbohydrate and energy metabolism. Sucrose synthase (spot 7349) involved in sugar metabolism was reduced in salt-treated plants. However, both transketolase (TK) (spots 8865 and 7410) in the pentose
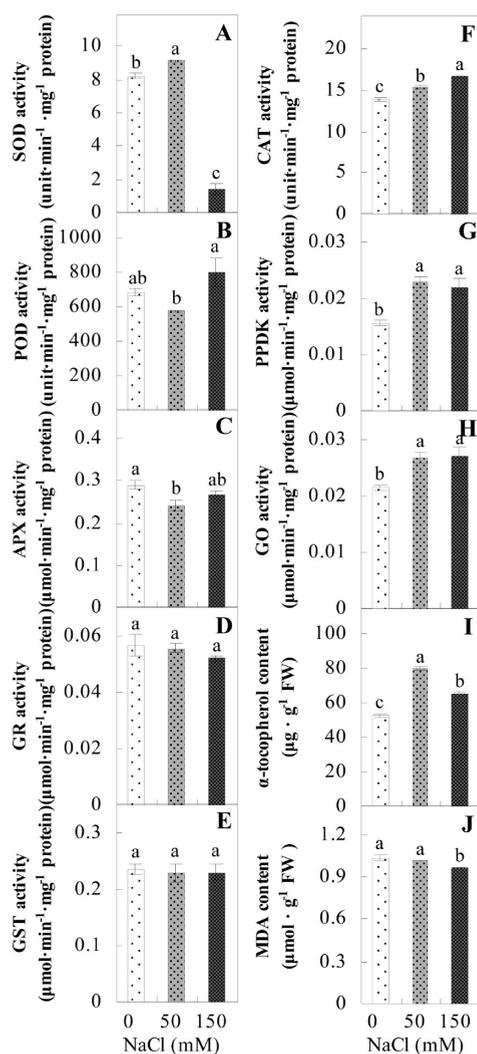
Figure 5. Effect of salinity on the activities of antioxidant-related enzymes and contents of α-tocopherol and malondialdehyde (MDA) in *P. tenuiflora* leaves: (A) superoxide dismutase (SOD); (B) peroxidase (POD); (C) ascorbate peroxidase (APX); (D) glutathione reductase (GR); (E) glutathione *S*-transferase (GST); (F) catalase (CAT); (G) pyruvate orthophosphate dikinase (PPDK); (H) glycolate oxidase (GO); (I) α-tocopherol content; (J) MDA content. The values were determined after plants were treated with 0, 50, and 150 mM NaCl for 7 days and are presented as means ± SE (n = 3). The different small letters indicate significant difference ($p < 0.05$) in different treatments.

phosphate pathway (PPP) and aconitate hydratase (AH) (spot 7316) in the tricarboxylic acid (TCA) cycle showed increased expression in salt-treated plants. Interestingly, the changes in the abundance of ATP synthases and NADH dehydrogenase subunits were not uniform. Six ATP synthases (spots 7624, 7632, 8715, 8320, 8016, and 8550) decreased, but two (spots 8931 and 7701) increased in expression. Similarly, one NADH dehydrogenase subunit (spot 7886) decreased, but the other (spot 7378) was increased in abundance.

Twenty protein IDs were involved in transcription and protein metabolism, including transcription-related (1), protein synthesis (2), protein folding and transport (9), and protein degradation (8). Most of the proteins were reduced in salt-treated plants, such as RNA recognition motif (spot 8479), initiation factor 4F p28 (spot 8420), translationally controlled tumor protein
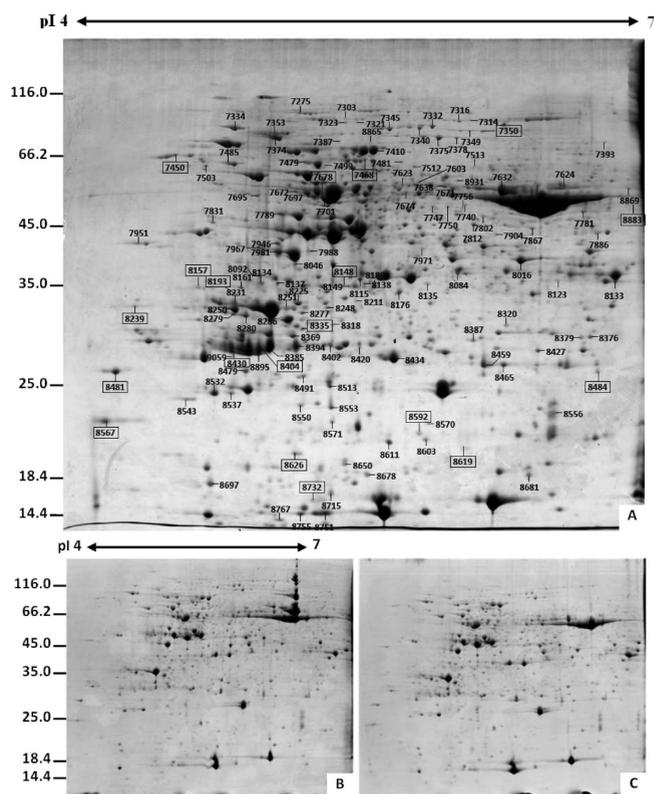

Figure 6. Coomassie Brilliant Blue (CBB)-stained 2 DE gel. Protein was extracted from leaves of *P. tenuiflora* under NaCl conditions for 7 days and separated on 24 cm IPG strips (pH 4—7 linear gradient) using isoelectric focusing (IEF) in the first dimension, followed by 12.5% SDS-PAGE gels in the second dimension. Spot numbers indicate the 138 identified spots, including 93 spots with a single protein each, 26 spots with more than one proteins each, and 19 spots with *de novo* sequenced proteins/peptides (squared). Please refer to Tables 1, 2, and Supporting Information Table S1. Molecular mass (MM) in kilodaltons and p*I* of proteins are indicated on the left and top, respectively. (A) 0 mM NaCl; (B) 50 mM NaCl; (C) 150 mM NaCl.

homologue (spot 8543), cytosolic HSP90 (spots 7374 and 7353), protein disulfide isomerase precursor (PDI) (spot 7485), and several proteasome subunits (spots 7479, 8379, 8376, 8402, 8611, and 7831). A few proteins increased in abundance in salt-treated plants, especially under 50 mM NaCl treatment, including AAA ATPases associated with a wide variety of cellular activities (spots 7345, 7340, 7332, and 7314), aminopeptidase N (spot 7323) and oligopeptidase A (spot 7387). In addition, we also found some proteins involved in metabolism (11), signaling (8), membrane and transport (3), and six of unknown function. Most of the proteins decreased in abundance under salt conditions (Table 1).

■ DISCUSSION

Growth Reduction Is an Adaptive Feature of *P. tenuiflora* under Salt Treatment

The level of tolerance and growth reduction varied widely among different plant species. Halophytes commonly exhibit more tolerance than glycophytes.[5] However, the less-tolerant halophytes grow better on nonsalinized soil. When growing under salt condition, they usually reduce their growth to cope with salinity.[5,23] The reduction in growth can save energy cost, reduce ROS production, decrease amino acid demand for protein

Table 1. Proteins and Their Relative Changes in Leaves of *P. tenuiflora* under Salt Treatment

Spot No. [a]	Protein name [b]	Plant Species [c]	gi Number [d]	Thr. MW(Da) /pI [e]	Exp. MW(Da) /pI [f]	Cov (%) [g]	Sco [h]	QM [i]	V%±SE [j] NaCl (mM) 0 50 150
Photosynthesis (15)									
8434	chlorophyll a/b binding protein	*Oryza sativa* (indica cultivar-group)	149392115	20,889 /5.81	25,603 /5.82	9	95	2	
8895	chlorophyll a/b binding protein	*Amaranthus hypochondriacus*	398599	28,709 /5.68	26,163 /5.17	15	189	4	
8385	chlorophyll a/b binding protein	*Hedera helix*	12582	20,759 /4.83	26,871 /5.24	9	78	2	
8251	chloroplast oxygen-evolving enhancer protein 1 (OEE)	*Leymus chinensis*	147945622	34,719 /6.08	31,185 /5.34	33	584	12	
7946	magnesium chelatase 40-kDa subunit	*H. vulgare subsp. vulgare*	148763638	45,516 /5.4	40,070 /5.29	30	573	13	
8459	carbonic anhydrase, chloroplast precursor	*H. vulgare*	729003	35,736 /8.93	25,200 /6.39	12	151	5	
8650	RubisCO large subunit	*Pentas lanceolata*	294117	53,478 /6.13	17,376 /5.59	11	171	5	
8603	RubisCO large subunit	*Psathyrostachys huashanica*	51859667	53,454 /6.13	19,031 /6.02	6	80	3	
7781	RubisCO large subunit	*Sparrmannia ricinocarpa*	4995862	52,664 /6.1	53,390 /7.00	22	365	9	
8755	RubisCO small subunit	*Avena vaviloviana*	3901432	19,072 /8.6	14,424 /5.42	19	178	5	
7789	ribulose-bisphosphate carboxylase activase	*Hordeum vulgare*	100614	47,496 /5.64	52,189 /5.31	19	378	7	
8046	sedoheptulose-1,7-bisphosphatase, chloroplast precursor (SBPase)	*T. aestivum*	1173347	42,547 /6.04	36,915 /5.39	10	158	4	
7981	phosphoribulokinase (PRK)	*Triticum aestivum*	21839	45,406 /5.84	38,685 /5.29	21	342	9	
8211	thiazole requiring (THI1), containing COG1635 Thi4 (Ribulose 1,5-bisphosphate synthetase, converts PRPP to RuBP, flavoprotein) family domain	*Arabidopsis thaliana*	15239735	36,755 /5.82	32,126 /5.62	3	108	2	
8869	AT4g13930, containing cd00378 serine-glycine hydroxymethyltransferase (SHMT) domain	*A. thaliana*	11762130	52,220 /7.12	64,390 /6.96	9	263	7	
Stress and defense (15)									
8369	ascorbate peroxidase	*H. vulgare*	15808779	27964 /5.1	28,000 /5.38	23	291	4	
8387	Os03g0285700, containing cd00691 ascorbate peroxidase domain	*O. sativa* (japonica cultivar-group)	115452337	27,253 /5.42	27,579 /6.32	12	164	3	
8570	cytosolic glutathione peroxidase	*T. monococcum*	34334012	18,613 /6.73	20,308 /6.04	16	111	3	
8427	glutathione S-transferase I (GST-I)	*Z. mays*	121695	24,034 /5.44	26,525 /6.72	17	173	3	
8537	hypothetical protein, containing cd03015 PRX_Typ2cys domain	*H. vulgare*	1076722	27,415 /5.87	22,663 /5.00	9	91	2	
8279	hypothetical protein, containing cd03015 PRX_Typ2cys domain	*H. vulgare*	1076722	27,415 /5.87	30,453 /5.02	9	71	2	

Table 1. Continued

Spot No. [a]	Protein name [b]	Plant Species [c]	gi Number [d]	Thr. MW(Da) /pI [e]	Exp. MW(Da) /pI [f]	Cov (%) [g]	Sco [h]	QM [i]	V%±SE [j] NaCl (mM) 0 50 150
8697	thioredoxin M-type, chloroplast precursor	T. aestivum	11135474	19,690 /8.67	16,120 /4.88	18	178	4	
7747	tocopherol cyclase (VTE1)	T. aestivum	91694297	52,497 /6.77	55,973 /6.07	5	111	3	
8084	ferredoxin-NADP(H) oxidoreductase (FNR)	T. aestivum	20302473	40,491 /6.92	35,648 /6.22	22	479	12	
9059	Os02g0328300, containing cd00322 ferredoxin reductase (FNR) domain	O. sativa (japonica cultivar-group)	115445869	30,791 /5.44	25,938 /5.02	7	100	2	
8277	putative glyoxalase	O. sativa (japonica cultivar-group)	46485858	29,720 /4.99	30,611 /5.42	32	502	13	
8248	hypothetical protein OsI_06754, containing PRK10291 glyoxalase I domain	O. sativa (indica cultivar-group)	125538981	41,635 /6.86	31,255 /5.54	14	303	6	
7951	probable plastid lipid associated protein 3, chloroplast precursor	O. sativa Japonica Group	62900689	40,073 /4.42	40,000 /4.42	3	119	2	
7503	Os02g0257300, containing cd01522 rhodanese homology domain 1 (RHOD_1) domain	O. sativa (japonica cultivar-group)	115445387	48,373 /5.05	75,504 /4.85	2	85	2	
7802	Os03g0163300, containing pfam02852 pyridine nucleotide disulphide oxidoreductase, dimerisation domain	O. sativa (japonica cultivar-group)	115450913	60557 /7.25	51,283 /6.38	7	191	4	
Carbohydrate and energy metabolism (15)									
7349	sucrose synthase	Bambusa oldhamii	17980243	92,593 /6.03	97,063 /6.30	17	657	15	
8865	putative transketolase	O. sativa (japonica cultivar-group)	28190676	80,549 /6.12	89,022 /5.68	11	393	9	
7410	putative transketolase	O. sativa (japonica cultivar-group)	28190676	80,549 /6.12	83,690 /5.70	13	531	10	
7316	putative aconitate hydratase 1	Sorghum bicolor	92429669	107,541 /6.63	103,673 /6.23	4	202	5	
7624	ATP synthase CF1 alpha subunit	T. aestivum	14017569	55,318 /6.11	65,370 /6.88	21	466	10	
7632	ATP synthase CF1 alpha subunit	T. aestivum	14017569	55,318 /6.11	62,218 /6.50	33	746	12	
8715	ATP synthase alpha subunit	T. aestivum	552976	55,287 /5.94	15,571 /5.55	5	122	3	
8931	ATP synthase alpha subunit	T. aestivum	552976	55,287 /5.94	68,118 /6.21	6	151	3	
8320	ATP synthase alpha subunit	T. aestivum	552976	55,287 /5.94	29,211 /6.52	13	377	7	
7701	ATP synthase beta subunit	T. aestivum	525291	59,326 /5.56	59,300 /5.53	50	1364	27	
8016	ATP synthase subunit gamma, chloroplast precursor	Z. mays	110278822	40,107 /8.44	37,468 /6.61	12	225	5	
8550	Os07g0495200, containing pfam02823 ATP synthase, delta/epsilon chain domain	O. sativa (japonica cultivar-group)	115472191	21,200 /5.72	21,640 /5.42	9	111	2	

Table 1. Continued

Spot No. [a]	Protein name [b]	Plant Species [c]	gi Number [d]	Thr. MW(Da) /pI [e]	Exp. MW(Da) /pI [f]	Cov (%) [g]	Sco [h]	QM [i]	V%±SE [j] NaCl (mM) 0 50 150
7378	Os03g0713400, containing cd02773 NADH dehydrogenase domain	O. sativa (japonica cultivar-group)	115454943	82,148 /5.86	92,130 /6.22	19	609	16	
7886	NADH dehydrogenase subunit 7	Beta vulgaris subsp. vulgaris	87248044	45,190 /6.36	43,964 /6.79	10	158	4	
8149	Os08g0379400, containing pfam00107 zinc-binding dehydrogenase domain	O. sativa (japonica cultivar-group)	115476190	39,672 /7.63	33,967 /5.60	4	106	2	
Metabolism (11)									
7971	caffeic acid O-methyltransferase	Festuca arundinacea	14578613	39,087 /5.47	39,205 /6.00	5	94	2	
7303	pyruvate, orthophosphate dikinase (PPDK)	Zea mays	168586	103,356 /5.71	105,685 /5.59	6	263	5	
8176	cysteine synthase	T. aestivum	585032	34,207 /5.48	33,169 /5.86	32	388	11	
8137	spermidine synthase	A. thaliana	2821961	32,710 /4.97	34,272 /5.29	9	130	2	
8678	BRI1-KD interacting protein 114, containing cd04413 nucleoside diphosphate kinase group I-like domain	O. sativa (japonica cultivar-group)	42733490	16,703 /5.79	16,700 /5.66	21	167	3	
8225	putative inorganic pyrophosphatase	O. sativa (japonica cultivar-group)	46805452	31,762 /5.8	31,723 /5.40	6	90	2	
8135	Os08g0327400, containing PRK06300 enoyl-(acyl carrier protein) reductase domain	O. sativa (japonica cultivar-group)	115475922	39,277/ 8.81	34,272 /6.03	12	169	4	
7904	Os05g0125500, containing cd01156 Isovaleryl-CoA dehydrogenase (IVD) domain	O. sativa (japonica cultivar-group)	115461843	45,073 /6.52	43,353 /6.46	4	112	2	
7512	Os08g0559600, containing PRK00911 dihydroxy-acid dehydratase domain	O. sativa (japonica cultivar-group)	115477815	64,237 /7.12	75,090 /5.95	5	174	3	
8681	unknown protein, containing cd04623 CBS_pair_10 domain	Z. mays	53771902	32,079 /9.47	16,664 /6.66	6	105	3	
8318	hypothetical protein OsI_13473, containing cd01910 Wali7 domain	O. sativa (indica cultivar-group)	125545688	31,122 /6.99	29,298 /5.55	7	83	2	
Transcription related (1)									
8479	Os09g0279500, containing cd00590 RRM (RNA recognition motif) domain	O. sativa (japonica cultivar-group)	115478330	26,779 /8.53	24,571 /5.09	10	132	3	
Protein synthesis (2)									
8420	initiation factor (iso) 4F p28 subunit	T. aestivum	170753	23,736 /5.35	26,813 /5.64	10	111	2	
8543	translationally-controlled tumor protein homolog (TCTP)	Pseudotsuga menziesii	9979193	18,883 /4.68	22,145 /4.73	10	107	2	
Protein folding and transport (9)									
7374	cytosolic HSP90	H. vulgare	32765549	80,654 /4.96	92,383 /5.27	31	121	22	
7353	cytosolic HSP90	H. vulgare	32765549	80,654 /4.96	95,477 /5.27	16	665	12	
7485	protein disulfide-isomerase precursor (PDI)	T. aestivum	1709620	56,726 /4.99	76,969 /4.99	7	158	4	

Table 1. Continued

Spot No.[a]	Protein name[b]	Plant Species[c]	gi Number[d]	Thr. MW(Da)/pI[e]	Exp. MW(Da)/pI[f]	Cov (%)[g]	Sco[h]	QM[i]	V%±SE[j] NaCl (mM) 0 50 150
7345	OSJNBa0039C07.4, containing cd00009 AAA ATPases domain	O. sativa (japonica cultivar-group)	38347158	98,550 /5.79	98,000 /5.80	38	180	36	
7340	OSJNBa0039C07.4, containing cd00009 AAA ATPases domain	O. sativa (japonica cultivar-group)	38347158	98,550 /5.79	98,540 /5.98	40	195	39	
7332	Os12g0230100, containing cd00009 AAA ATPases domain	O. sativa (japonica cultivar-group)	115487910	102,068 /6.62	99,628 /6.06	35	163	33	
7314	Os03g0426900, containing cd00009 AAA ATPases domain	O. sativa (japonica cultivar-group)	115453619	109,146 /6.25	104,244 /6.30	4	127	4	
8491	OSJNBa0039C07.4, containing cd00009 AAA ATPases domain	O. sativa (japonica cultivar-group)	38347158	98,550 /5.79	24,131 /5.43	10	430	7	
8556	OSJNBa0039C07.4, containing cd00009 AAA ATPases domain	O. sativa (japonica cultivar-group)	38347158	98550 /5.79	20,978 /6.83	10	369	8	
Protein degradation (8)									
7323	putative aminopeptidase N	O. sativa (japonica cultivar-group)	42408435	98,597 /5.42	102,964 /5.60	5	144	4	
7387	Os02g0830100, containing cd06456 oligopeptidase A domain	O. sativa (japonica cultivar-group)	115450022	86,506 /5.76	90,501 /5.58	7	239	6	
7479	putative FtsH-like protein Pftf precursor	O. sativa (japonica cultivar-group)	52075838	72,607 /5.54	77,605 /5.44	8	310	6	
8379	20S proteasome subunit alpha 3	Lolium perenne	14039743	21,016 /6.41	27,839 /6.99	18	135	4	
8376	proteasome subunit alpha type 6, putative, expressed	O. sativa (japonica cultivar-group)	108706511	32,472 /7.05	27,919 /7.04	23	314	7	
8402	Os02g0634900, containing cd03750 proteasome alpha type 2 domain	O. sativa (japonica cultivar-group)	115447473	25,828 /5.39	27,125 /5.55	25	294	6	
8611	Os02g0634900, containing cd03750 proteasome alpha type 2 domain	O. sativa (japonica cultivar-group)	115447473	25,828 /5.39	18,839 /5.80	14	125	3	
7831	Os06g0167600, containing cd03752 proteasome alpha type 4 domain	O. sativa (japonica cultivar-group)	115466646	27,180 /6.44	48,406 /4.89	7	94	2	
Signaling(8)									
8280	14-3-3	H. vulgare subsp. vulgare	83271056	28,742 /4.8	30,362 /5.09	26	428	8	
8250	14-3-3 protein homolog	H. vulgare	100554	29,361 /4.83	30,886 /5.03	58	876	20	
8532	14-3-3 protein homolog	H. vulgare	100554	29,361 /4.83	22,614 /4.90	34	453	9	
8231	14-3-3 protein homolog	H. vulgare	100554	29,361 /4.83	31,841 /5.02	38	624	11	
7375	TaWIN2, containing pfam00244 14-3-3 protein domain	T. aestivum	9798605	28,794 /4.8	91,752 /6.10	29	222	5	
8465	TaWIN2, containing pfam00244 14-3-3 protein domain	T. aestivum	9798605	28,794 /4.8	25,181 /6.51	17	97	3	
7740	GDP dissociation inhibitor protein (OsGDI1)	O. sativa	2384758	50,069 /5.69	56,861 /6.27	9	204	4	
8134	alpha-SNAP	H. vulgare subsp. vulgare	32308080	12,621 /4.93	34,323 /5.19	33	175	4	

Table 1. Continued

Spot No. [a]	Protein name [b]	Plant Species [c]	gi Number [d]	Thr. MW(Da) /pI [e]	Exp. MW(Da) /pI [f]	Cov (%) [g]	Sco [h]	QM [i]	V%±SE [j] NaCl (mM) 0 50 150
	Membrane and transport (3)								
7672	Vacuolar ATP synthase subunit B2	*H. vulgare*	2493132	53,806 /5.12	62,905 /5.39	38	806	16	
7867	Vacuolar ATP synthase subunit B2	*H. vulgare*	2493132	53,806 /5.12	45,850 /6.68	9	191	4	
7393	Os03g0271200, containing pfam01103 Bac_surface_Ag Surface antigen domain	*O. sativa* (japonica cultivar-group)	115452177	88,145 /8.5	89,390 /7.13	6	258	6	
	Unknown (6)								
8767	Os01g0144100, containing pfam00805 pentapeptide repeats (8 copies) domain	*O. sativa* (japonica cultivar-group)	115434488	20,676 /6.71	14,105 /5.30	16	140	3	
8513	Os05g0401100, containing pfam04536, domain of unknown function (DUF477)	*O. sativa* (japonica cultivar-group)	115463773	31,807 /8.47	23,226 /5.55	7	107	2	
8553	Os05g0401100, containing pfam04536, domain of unknown function (DUF477)	*O. sativa* (japonica cultivar-group)	115463773	31,807 /8.47	21,484 /5.55	7	101	2	
8571	hypothetical protein, containing pfam10674, domain of unknown function (DUF2488)	*Vitis vinifera*	147818338	25,560 /7.85	20,337 /5.55	5	98	2	
8161	Os02g0117100, containing pfam09353, domain of unknown function (DUF1995)	*O. sativa* (japonica cultivar-group)	115443809	42,207 /6.67	33,716 /5.07	2	100	2	
8138	unknown protein, No putative conserved domains have been detected	*O. sativa* (japonica cultivar-group)	22758313	35,437 /5.57	34,348 /5.65	5	104	2	

[a] Assigned spot number as indicated in Figure 6. [b] The name and functional categories of the proteins identified by ESI Q-TOF MS. [c] The plant species that the peptides matched from. [d] Database accession numbers from NCBInr. [e,f] Theoretical (e) and experimental (f) mass (kDa) and pI of identified proteins. Experimental values were calculated using Image Master 2D Platinum Software. Theoretical values were retrieved from the protein database. [g] The amino acid sequence coverage for the identified proteins. [h] The Mascot score obtained after searching against the NCBInr database. [i] The number of unique peptides identified for each protein. [j] The mean values of protein spot volumes relative to total volume of all the spots. Three NaCl treatments (0, 50, and 150 mM) were performed. Error bars indicate ± standard error (SE).

synthesis, and thereby provide more free amino acids for osmotic adjustment.[23,50] In this study, under moderate NaCl conditions, the fresh weight and shoot length of *P. tenuiflora* declined slightly (Figure 1A,B). In addition, our proteomics results revealed that 80 out of the 107 protein IDs reduced in levels under salt treatment (Table 1, Supporting Information Figure S2B). Especially, 15 decreased proteins function in transcription (e.g., RNA recognition motif), protein synthesis (e.g., initiation factor 4F), protein folding (such as HSP90 and PDI), and protein degradation (proteasome subunit alpha and FtsH-like protein) (Tables 1 and 2). A similar gene expression pattern in *P. tenuiflora* under 48 h NaHCO$_3$ treatment has also been previously observed.[51] The decline in gene expression and protein synthesis has also been observed in previous studies using barley,[52] *Prosopsis*,[53] wheat,[54] *Bruguiera parviflora*,[55] and *Aeluropus lagopoides*.[23] This implies that salinity-responsive protein biosynthesis/turnover contributed to the decline of global metabolism levels and growth.[23]

Osmotic Adjustment and Intracellular Ion Balance Are Important for Halophyte Salt Tolerance

Under salt treatment, plants generally reduce their water contents (WC) in the shoots as a rapid and economical approach in response to the increase in the external osmotic pressure. In *P. tenuiflora* leaves, the WC decreased slightly with the reduction of osmotic potential under NaCl treatment (Figures 1C and 3A). This is likely to be an adaptive feature in halophytes for accumulating osmolytes with minimum energy consumption.[56] In addition to the WC adjustment, plants accumulate organic solutes and inorganic ions in the cells for osmotic adjustment. The accumulated low molecular weight compatible organic solutes (e.g., proline, soluble sugar, and betaine) in cytoplasm can prevent dehydration by keeping a stable osmotic pressure but also protect macromolecules (e.g., proteins and nuclear acids) from degeneration.[26] In this study, the contents of proline, soluble sugar, and betaine in leaves were significantly increased under 150 mM salt (Figure 3B−D). This implies that the increase of compatible organic solutes is one of the major strategies to tolerate salinity in *P. tenuiflora*. In addition, the accumulation of inorganic ions (e.g., significant increase in Na$^+$ and Cl$^-$ contents) in *P. tenuiflora* with increasing salinity also contributed to osmotic adjustment to a certain extent (Figure 3E,L). Most accumulated inorganic ions have been compartmentalized into vacuoles to avoid ion toxicity in the cytosol.[57]

Accompanying Na$^+$ and Cl$^-$ increase for osmotic adjustment, *P. tenuiflora* re-established intracellular ionic balance in leaves.

Table 2. Proteins Identified by *de Novo* Sequencing and Their Relative Changes in Leaves from *P. tenuiflora* under Salt Treatment

Spot No.[a]	*de novo* sequenced peptide[b]	Matched/given protein name[c]	Species[d]/gi Number[e]	Thr. MW(Da)/pI[f]	Exp. MW(Da)/pI[g]	V%±SE[h] NaCl (mM) 0 50 150
7468	QDGLEEVRK	porphobilinogen deaminase (Metabolism)	*Puccinia graminis* f. sp. tritici CRL 75-36-700-3/309306794	50,210/5.80	76,026/5.57	
8481	WLLDELAK	heat shock protein DnaJ domain protein (Protein folding and transport)	*Spirochaeta thermophila* DSM 6578/315185537	28,065/9.87	32,519/4.34	
8883	LACTLPR	hypothetical protein Franean1_0062, containing COG2856 predicted Zn peptidase domain (Protein degradation)	*Frankia* sp. EAN1pec/158311928	42,630/7.92	66,652/6.98	
8592	LALEEVK	unnamed protein product (Unknown)	*Oikopleura dioica*/313231961	93,989/5.82	17,616/5.85	
7350	NPVLLAQTLTMR	PuDnSP1	-	-	82,714/6.19	
7678	AFKELVEGREK	PuDnSP2	-	-	68,813/5.35	
8148	FCGQANPPR VAAAALNPVDSK	PuDnSP3	-	-	50,509/5.46	
8157	FSGVTAQGERK	PuDnSP4	-	-	50,169/4.72	
8193	DDPHTYSPK QYSMNVAAVVK	PuDnSP5	-	-	48,628/4.90	
8239	YLLGLTQEQR	PuDnSP6	-	-	46,268/4.43	
8335	SSGTSYPNVLK RPFVPEPK	PuDnSP7	-	-	40,959/5.24	
8430	ANVANPASTTFNWHK MAQGEEGPNFK	PuDnSP8	-	-	36,364/4.88	
8484	KSSVEGVEVK	PuDnSP9	-	-	32,620/6.79	
8619	SSGTSYPDLVK	PuDnSP10	-	-	14,660/6.09	

[a] Assigned spot number as indicated in Figure 6. [b] *De novo* sequenced peptides as indicated in Supporting Information Figure S2. [c] The name and functional categories of the matched proteins by BLAST. [d] The plant species that the peptides matched from. [e] Database accession numbers from NCBInr. [f,g] Theoretical (f) and experimental (g) mass (kDa) and pI of identified proteins. Experimental values were calculated using Image Master 2D Platinum Software. Theoretical values were retrieved from the protein database. [h] The mean values of protein spot volumes relative to total volume of all the spots. Three NaCl treatments (0, 50, and 150 mM) were performed. Error bars indicate ± standard error (SE).

Our results show that the dynamics of cations (Na^+, K^+, Ca^{2+}, Mg^{2+}, and NH_4^+) and anions (Cl^-, NO_3^-, and PO_4^{3-}) in leaves plays a key role on ion balance adjustment (Figure 3). K^+ is the essential ion for various physiological processes, especially for protein synthesis and enzyme activation. *P. tenuiflora* was found to keep significantly high cytoplasmic K^+/Na^+ ratios in leaves under salt treatment (Figure 3E−G) compared to wheat,[30] indicating maintenenance of cytoplasmic metabolism and ion homeostasis under salt condition. In addition, the increase of Na and K on leaf surface implied that Na^+ and K^+ were secreted onto leaf surface and the process intensified under salt treatment (Figure 3H,I).[31] However, the Na^+ secretion was minimal considering the entire plant Na^+ concentration[30] and was very small in comparison to other salt-secreting halophytes (e.g., *Spartina anglica*, *Limonium vulgare*, and *Glaux maritime*).[30,58] Thus, secretion of Na^+ might mainly serve to reflect light (discussed below) but not for ion balance.[30,59] It was also found the concentrations of bivalent cations (Mg^{2+} and Ca^{2+}) were stable or increased in leaves of *P. tenuiflora* under salt treatment (Figure 3J,K). Mg^{2+} is a key component of chlorophyll, and Ca^{2+} is important for membrane stability, cell wall construction, and signal transduction. The increased/stable levels of Ca^{2+} and Mg^{2+} in *P. tenuiflora* leaves allow for stabilization of photosynthesis, cell structure, and signaling. Ca^{2+} and Mg^{2+} accumulation was also found to be increased in a naturally alkali-resistant halophyte *K. sieversina*[56] but decreased in a subtropical perennial halophyte
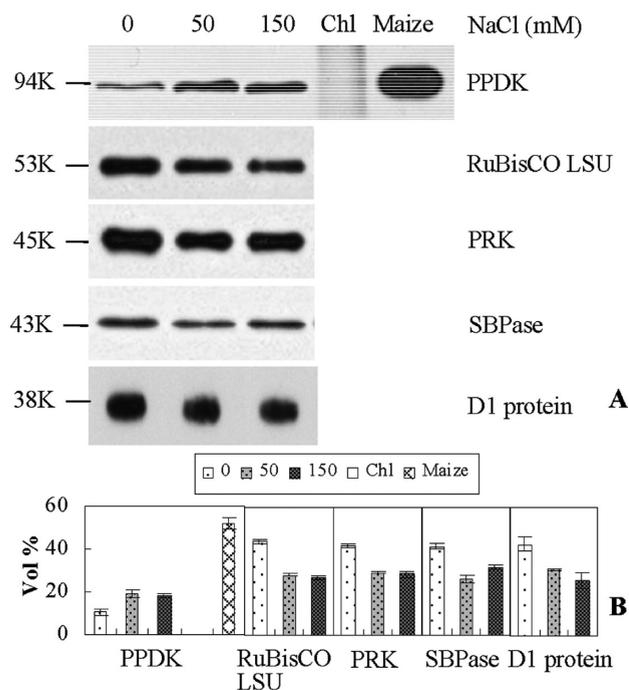
Figure 7. Western blot of pyruvate orthophosphate dikinase (PPDK), ribulose-1,5-bisphosphate carboxylase large unit (RuBisCO LSU), phosphoribulokinase (PRK), sedoheptulose-1,7-bisphosphatase (SBPase), and D1 protein in leaves from *P. tenuiflora* under salt treatment. (A) Western blot image of PPDK, RuBisCO LSU, PRK, SBPase, and D1 protein. (B) Relative abundance of the five proteins shown in panel A.

Atriplex griffithii var. *stocksii* under salt treatment.[60] Furthermore, in this study Cl$^-$ concentration significantly increased in a pattern similar to Na$^+$ (Figure 3L). This is a common feature in halophytes (e.g., *Kochia sieversiana*),[56] salt-tolerant species (e.g., *Oryza sativa* IR651),[61] and salt-sensitive species (e.g., sorghum, barley, and wheat).[62] PO$_4$$^{3-}$ concentration also increased in *P. tenuiflora* leaves under salt treatment (Figure 3M). In contrast, NO$_3$$^-$ concentration decreased (Figure 3N). These results are consistent with previous reports on *P. tenuiflora*[26] and the salt-tolerant sunflower (*Helianthus annuus*).[63] All these imply that the various inorganic anions in diverse plant species differ in their contribution to maintaining ion balance.

Photosynthesis Reduced under Salt Treatment

Stomatal aperture is sensitive to transient salt-perturbed water conditions, although various osmotic adjustments take place immediately in response to salinity. The declined stomatal conductance led to the decreased leaf intercellular CO$_2$ levels and consequently the decrease of photosynthesis.[3,64,65] In *P. tenuiflora*, Pn, Gs, Ci, and Tr all gradually declined with the increase of NaCl concentrations, and WUE increased under 150 mM NaCl treatment (Figure 4A−E). This was further supported by quantitative proteomics and immunoblot results that revealed a decrease in abundance of some photosynthetic enzymes under salt treatment. Five Calvin cycle-related enzymes reduced their expression levels, including RuBisCO LSU/SSU, RuBisCO activase, CA, SBPase, and PRK (Table 1, Figure 8), and three of them (RuBisCO, SBPase, and PRK) were confirmed to be decreased by Western blot analysis (Figure 7). This suggests the reduction of RuBP regeneration and inhibition of Calvin cycle activity

(Figure 8). This is consistent with findings in halophyte C4 plant *A. lagopoides*.[23] On the contrary, some photosynthesis-related enzymes (e.g., RuBisCO LSU and RuBisCO activase) were increased in *S. europaea*[19] and wild halophytic rice (*Porteresia coarctata*).[24] This implies that diverse salt-responsive CO$_2$ assimilation strategies are utilized in various species of monocotyledonous halophyte C3 plant,[24] C4 plant *A. lagopoides*,[23] and dicotyledonous halophyte *S. europaea*.[19]

We observed the reduction of light reactions represented by the decrease of Fv/Fm, Fv'/Fm', qL, ETR, and φPSII under salt treatment (Figure 4G−K). This is consistent with monocotyledonous *Paspalum vaginatum*.[66] Down-regulation of CAB and D1 proteins in *P. tenuiflora* would decrease the size of antenna and reduce light absorption (Table 1, Figure 7).[59] In contrast, in dicotyledonous halophyte *Suaeda salsa*[67] and *S. aegyptiaca*,[20] the Fv/Fm, Fv'/Fm', qL, and φPSII were not affected by salt,[67] and some PSII assembly/stabilization-related proteins (e.g., D2 protein) accumulated under salt treatment.[20] Besides, C4 plant *A. lagopoides* was inclined to harvest more light under salt condition due to the increase of CAB of LHCII type III under 150 mM NaCl treatment.[23] These results suggest that species in different taxonomic groups of halophytes utilize different light reaction strategies to cope with salinity.

Unique Mechanisms of *P. tenuiflora* in Coping with Oxidative Stress

Generally, blockage in photosynthesis would enhance the production of ROS in cells, which can cause oxidative damage to lipids, proteins, and DNA, thereby affecting the integrity of cellular membranes, enzyme activities, and the function of photosynthetic apparatus. However, we did not observe any significant oxidative damage in *P. tenuiflora* under salt treatment. The content of MDA, an indicator of the lipid peroxidation, did not show significant changes under salt condition (Figure 5J), suggesting little lipid peroxidation. In addition, the ROS scavenging system was not consistently up-regulated. SOD, an important antioxidant enzyme constituting the first line of defense against oxidative stress,[68] slightly increased its activity under 50 mM NaCl but dramatically decreased under 150 mM NaCl treatment (Figure 5A). Such salinity responses were also observed in our previous study of *P. tenuiflora* growing under high concentrations of NaCl and Na$_2$CO$_3$.[32] More importantly, four key enzymes in Halliwell−Asada pathway, POD, APX, GR, and GST, appeared stable in their activities under salt treatment (Figure 5B−E). Furthermore, our proteomics results revealed that the expression levels of five antioxidative enzymes (APX, Prx, Trx, GPX, and GST) were all decreased under salinity conditions (Table 1, Figure 8). However, the dynamics of antioxidative enzymes responsive to salinity is different in other species.[3,19,23,68] This suggest that *P. tenuiflora* did not mainly rely on the Halliwell−Asada pathway in dealing with oxidative stress.

One of the alternative antioxidative mechanisms in *P. tenuiflora* leaves is the enhancement of photorespiration. Under salt treatment, reduced water availability and stomatal aperture, as well as the reduction of CO$_2$ assimilation, could lead to photorespiration (Figures 1C and 4A−C,F).[59] Furthermore, the gradual increase in the activities of GO and CAT (Figures 5F,H and 8) could enhance the oxidation of glycolate and scavenging of H$_2$O$_2$ in peroxisomes during the photorespiratory process.[68] In addition, the increased expression of SHMT (Table 1, Figure 8) suggests activation of the photorespiratory pathway in salinity tolerance.[69] Besides photorespiration, enhancement of thermal dissipation
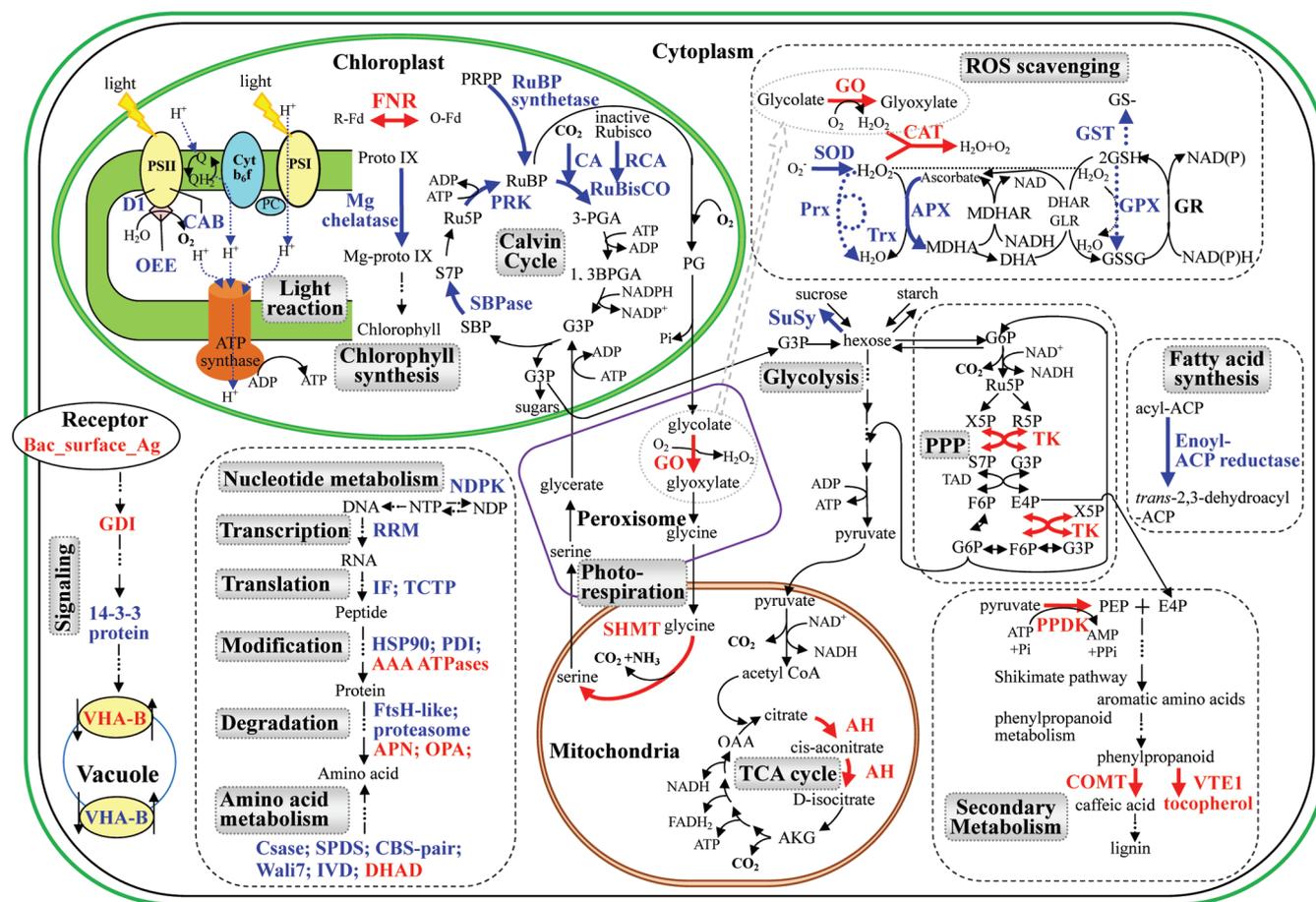
Figure 8. Schematic presentation of systematic salt tolerance mechanisms in *P. tenuiflora*. The identified proteins were integrated into subcellular locations and pathways. Protein expression patterns were shown by marking the protein names and reactions in red (increased) or blue (decreased) words and arrows, respectively. Abbreviations: 1,3BPGA, 1,3-bisphosphoglycerate; 3-PGA, 3-phosphoglycerate; AAA ATPases, ATPases associated with a wide variety of cellular activities; ACP, acyl carrier protein; ADP, adenosine diphosphate; AH, -ketoglutarate; AMP, adenosine monophosphate; APN, aconitate hydratase; AKG, aminopeptidase N; APX, ascorbate peroxidase; ATP, adenosine-triphosphate; CA, carbonic anhydrase; CAB, chlorophyll a/b binding protein; CAT, catalase; CBS, cystathionine beta-synthase; COMT, caffeic acid O-methyltransferase; Csase, cysteine synthase; D1, D1 protein; DHA, dehydroascrobate; DHAD, dihydroxy-acid dehydratase; DHAR, DHA reductase; E4P, erythrose-4-phosphate; F6P, fructose-6-phosphate; FADH$_2$, reduced flavin adenine dinucleotide; FNR, ferredoxin-NADP reductase; G3P, glyceraldehydes-3-phosphate; G6P, glucose-6-phosphate; GDI, GDP dissociation inhibitor protein; GLR, glutaredoxin; GO, glycolate oxidase; GPX, glutathione peroxidase; GR, glutathione reductase; GSH, reduced glutathione; GSSG, oxidized glutathione; GST, glutathione S-transferase; HSP90, heat shock protein 90; IF, initiation factor; IVD, isovaleryl-CoA dehydrogenase; MDHA, monodehydroascorbate; MDHAR, MDHA reductase; Mg, magnesium; NAD$^+$/NADH, nicotinamide adenine dinucleotide; NADP$^+$/NADPH, nicotinamide adenine dinucleotide phosphate; NDPK, nucleoside diphosphate kinase; NDP, nucleoside diphosphate; NTP, nucleoside triphosphate; OAA, oxaloacetic acid; OEE, oxygen-evolving enhancer protein; O-Fd, oxidized ferredoxin; OPA, oligopeptidase A; PC, plastocyanin; PDI, protein disulfide-isomerase precursor; PEP, phosphoenolpyruvate; PG, phosphoglycolate; PPDK, pyruvate, orthophosphate dikinase; PPP, pentose phosphate pathway; PRK, phosphoribulokinase; Proto, protoporphyrin; PRPP, 5-phospho-D-ribose-1-pyrophosphate; Prx, peroxiredoxin; PSI, photosystem I; PSII, photosystem II; Q, quinone; R5P, ribose-5-phosphate; RCA, RuBisCO activase; REC, reactive electrophillic compounds; R-Fd, reduced ferredoxin; RRM, RNA recognition motif; Ru5P, ribulose-5-phosphate; RuBisCO, ribulose-1,5-bisphosphate carboxylase/oxygenase; RuBP, ribulose-1,5-bisphosphate; S7P, sedoheptulose-7-phosphate; SBP, sedoheptulose-1,7-bisphosphate; SBPase, sedoheptulose-1,7-bisphosphatase; SHMT, serine-glycine hydroxymethyltransferase; SOD, superoxide dismutase; SPDS, spermidine synthase; SuSy, sucrose synthase; TAD, transaldolase; TCA cycle, tricarboxylic acid cycle; TCTP, translationally controlled tumor protein homologue; TK, transketolase; Trx, thioredoxin; VTE1, tocopherol cyclase; VHA-B, vacuolar H$^+$ ATP synthase subunit B2; X5P, xylulose-5-phosphate.

could be another way to quench excess energy. In this study, thermal dissipation as estimated by NPQ showed a gradual increase with increasing salinity (Figure 4L), indicating dissipation of excess absorbed light energy to protect the photochemical apparatus. In addition, the ion secretion onto leaf surface evaluated by increase of Na and K contents under NaCl treatment (Figure 3H,I) was proposed to prevent excessive light absorption.[31,59] Furthermore, some metabolites may play antioxidative roles, e.g., α-tocopherol can scavenge ROS and protect

lipids from oxidation.[68,70] In salt-treated leaves, we found an increase in α-tocopherol content (Figure 5I) and increased expression of VTE1 in tocopherol synthesis (Table 1). Previous studies also revealed the enhancement of α-tocopherol and VTE1 in plants under various environmental stresses.[71,72] In addition to osmotic adjustment, some increased compatible solutes in *P. tenuiflora* leaves (e.g., proline, soluble sugars, and betaine) (Figure 3B−D) were also suggested to scavenge ROS and protect cellular components.[68,73] Moreover, a photosynthetic

enzyme, FNR, has been proposed to participate in a variety of redox pathways and has been confirmed to function in defense against oxidative damage.[74] The increase of FNR in *P. tenuiflora* leaves could enhance the redox function but not photosynthesis since photosynthesis was decreased under salt treatment (Table 1, Figures 4 and 8).

Energy and Secondary Metabolite Adjustment under Salinity

The increased levels of AH and TK implied that the TCA cycle and the PPP were increased under salinity (Table 1 and Figure 8).[75] Enhancement of the PPP has been found in several species in response to various stress conditions,[75−77] and our results are consistent with previous proteomic studies.[19,22,78] Enhancement of the PPP would provide more glyceraldehydes-3-phosphate (G3P), glucose-6-phosphate (G6P), NADPH, and erythrose-4-phosphate (E4P) that could be used to produce more ATP.[75,79] The increase of E4P also provides more immediate carbon substrates for the shikimate pathway leading to phenylpropanoid metabolism.[75] Indeed, caffeic acid *O*-methyltransferase (COMT) involved in phenylpropanoid metabolism was increased in salt-treated *P. tenuiflora* (Table 1, Figure 8). COMT catalyzes the multistep methylation reaction of hydroxylated monomeric lignin precursors.[80] Lignin is a biopolymer integrated into reticular cellulose structure in the cell wall and was shown to deposit in great amounts in tomato vascular tissues under salt stress.[81] Similar results of increased COMT expression was observed in maize under drought stress.[82] Another enzyme potentially involved in lignin biosynthesis was identified as PPDK. PPDK is known to catalyze the reversible conversion of pyruvate to phosphoenolpyruvate in C4 plant chloroplasts[83] and in some C3 plants.[84] PPDK has been found increase in rice roots under various stress conditions (e.g., drying, cold, high salt/mannitol, and low oxygen)[85] and is proposed to function in lignin biosynthesis via the shikimate pathway.[86] Here, in *P. tenuiflora* leaves with a typical C3 structure (Figure 2), we did not detect obvious PPDK immunoreaction in chloroplasts (Figure 7), but the abundance and activity of PPDK were increased under salinity treatment (Table 1, Figures 5G and 7). Together with the increase of COMT, we propose that the cytosolic PPDK in C3 plant *P. tenuiflora* leaves was involved in providing PEP for lignin biosynthesis to cope with salinity.[86] The increased lignification of tracheary elements under salt stress may compensate for the diminished bulk flow of water and solutes along the apoplastic pathway.[81] Detailed investigation on the mechanisms underlying PPDK regulation in salt tolerance is an important future research direction.

■ ASSOCIATED CONTENT

Ⓢ Supporting Information

Isoforms of NaCl responsive proteins, protein spots with multiple proteins identified in a single spot on 2D gels, and MS/MS spectra of *de novo* sequenced peptides. This material is available free of charge via the Internet at http://pubs.acs.org.

■ AUTHOR INFORMATION

Corresponding Author

*E-mail: daishaojun@hotmail.com; grsun@live.cn.

■ ACKNOWLEDGMENT

■ ABBREVIATIONS:

2DE, two-dimensional gel electrophoresis; φPSII, actual PSII efficiency; AH, aconitate hydratase; APX, ascorbate peroxidase; CA, carbonic anhydrase; CAB, chlorophyll a/b binding protein; CAT, catalase; Ci, concentration of intercellular CO_2; COMT, caffeic acid O-methyltransferase; E4P, erythrose-4-phosphate; ESI-Q-TOF, electrospray quadrupole time-of-flight; ETR, electron transport rate; FNR, ferredoxin-NADP(H) oxidoreductase; G3P, glyceraldehyde-3-phosphate; G6P, glucose-6-phosphate; GDI, GDP dissociation inhibitor; GO, glycolate oxidase; GPX, glutathione peroxidase; Gs, stomatal conductance; GST, glutathione S-transferase; HDR, heat dissipation rate; IDs, identities; LHC, light-harvesting complex; MDA, malondialdehyde; MS, mass spectrometry; OEE1, oxygen-evolving enhancer protein 1; PDI, protein disulfide isomerase precursor; PEP, phosphoenolpyruvate; Pn, net photosynthetic rate; POD, peroxidase; PPDK, pyruvate orthophosphate dikinase; PPP, pentose phosphate pathway; PRK, phosphoribulokinase; Prx, peroxiredoxin; PSI, photosystem I; PSII, photosystem II; qL, fraction of PSII centers that are "open"; qP, photochemical quenching; ROS, reactive oxygen species; RuBisCO activase, ribulose-bisphosphate carboxylase activase; RuBisCO LSU, ribulose 1,5-bisphosphate carboxylase large unit; RuBisCO SSU, ribulose 1,5-bisphosphate carboxylase small unit; RuBP, ribulose-1,5-bisphosphate; SBPase, sedoheptulose-1,7-bisphosphatase; SHMT, serine-glycine hydroxymethyltransferase; SOD, superoxide dismutase; TBST, Tris buffered saline with Tween; TCA, tricarboxylic acid; TK, transketolase; Tr, transpiration rate; Trx, thioredoxin-chloroplast precursor; VTE1, tocopherol cyclase; WC, water content; WUE, water usage efficiency

■ REFERENCES

(1) Munns, R.; Tester, M. Mechanisms of salinity tolerance. *Annu. Rev. Plant Biol.* **2008**, *59*, 651–681.

(2) Tuteja, N. Mechanisms of high salinity tolerance in plants. *Methods Enzymol.* **2007**, *428*, 419–438.

(3) Parida, A. K.; Das, A. B. Salt tolerance and salinity effects on plants: a review. *Ecotoxicol. Environ. Saf.* **2005**, *60* (3), 324–349.

(4) Wang, M. C.; Peng, Z. Y.; Li, C. L.; Li, F.; Liu, C.; Xia, G. M. Proteomic analysis on a high salt tolerance introgression strain of *Triticum aestivum/Thinopyrum ponticum*. *Proteomics* **2008**, *8* (7), 1470–1489.

(5) Glenn, E. P.; Brown, J. J.; Blumwald, E. Salt tolerance and crop potential of halophytes. *Crit. Rev. Plant Sci.* **1999**, *18* (2), 227–255.

(6) Flowers, T. J.; Colmer, T. D. Salinity tolerance in halophytes. *New Phytol.* **2008**, *179* (4), 945–963.

(7) Jia, G. X.; Zhu, Z. Q.; Chang, F. Q.; Li, Y. X. Transformation of tomato with the *BADH* gene from *Atriplex* improves salt tolerance. *Plant Cell Rep.* **2002**, *21* (2), 141–146.

(8) Li, Q. L.; Gao, X. R.; Yu, X. H.; Wang, X. Z.; An, L. J. Molecular cloning and characterization of betaine aldehyde dehydrogenase gene from *Suaeda liaotungensis* and its use in improved tolerance to salinity in transgenic tobacco. *Biotechnol. Lett.* **2003**, *25* (17), 1431–1436.

(9) Shen, Y. G.; Yan, D. Q.; Zhang, W. K.; Du, B. X.; Zhang, J. S.; Liu, Q.; Chen, S. Y. Novel halophyte EREBP0 AP2-type DNA binding protein improves salt tolerance in transgenic tobacco. *Acta Bot. Sin.* **2003**, *45* (1), 82–87.

(10) Majee, M.; Maitra, S.; Dastidar, K. G.; Pattnaik, S.; Chatterjee, A.; Hait, N. C.; Das, K. P.; Majumder, A. L. A novel salt-tolerant L-myo-inositol-1-phosphate synthase from *Porteresia coarctata* (Roxb.) Tateoka, a halophytic wild rice: molecular cloning, bacterial over-expression, characterization, and functional introgression into tobacco-conferring salt tolerance phenotype. *J. Biol. Chem.* **2004**, *279* (27), 28539–28552.

(11) Wong, C. E.; Li, Y.; Labbe, A.; Guevara, D.; Nuin, P.; Whitty, B.; Diaz, C.; Golding, G. B.; Gray, G. R.; Weretilnyk, E. A.; Griffith, M.; Moffatt, B. A. Transcriptional profiling implicates novel interactions between abiotic stress and hormonal responses in *Thellungiella*, a close relative of *Arabidopsis*. *Plant Physiol.* **2006**, *140* (4), 1437–1450.

(12) Zhang, Y.; Lai, J.; Sun, S.; Li, Y.; Liu, Y.; Liang, L.; Chen, M.; Xie, Q. Comparison analysis of transcripts from the halophyte *Thellungiella halophila*. *J. Integr. Plant Biol.* **2008**, *50* (10), 1327–1335.

(13) Wang, Z.; Li, P.; Fredricksen, M.; Gong, Z.; Kim, C. S.; Zhang, C.; Bohnert, H. J.; Zhu, J. K.; Bressan, R. A.; Hasegawa, P. M. Expressed sequence tags from *Thellungiella halophila*, a new model to study plant salt-tolerance. *Plant Sci.* **2004**, *166* (3), 609–616.

(14) Wong, C. E.; Li, Y.; Whitty, B. R.; Diaz-Camino, C.; Akhter, S. R.; Brandle, J. E.; Golding, G. B.; Weretilnyk, E. A.; Moffatt, B. A.; Griffith, M. Expressed sequence tags from the Yukon ecotype of *Thellungiella* reveal that gene expression in response to cold, drought and salinity shows little overlap. *Plant Mol. Biol.* **2005**, *58* (4), 561–574.

(15) Zhang, L.; Ma, X. L.; Zhang, Q.; Ma, C. L.; Wang, P. P.; Sun, Y. F.; Zhao, Y. X.; Zhang, H. Expressed sequence tags from a NaCl-treated *Suaeda salsa* cDNA library. *Gene* **2001**, *267* (2), 193–200.

(16) Zouari, N.; Ben Saad, R.; Legavre, T.; Azaza, J.; Sabau, X.; Jaoua, M.; Masmoudi, K.; Hassairi, A. Identification and sequencing of ESTs from the halophyte grass *Aeluropus littoralis*. *Gene* **2007**, *404* (1−2), 61–69.

(17) Jha, B.; Agarwal, P. K.; Reddy, P. S.; Lal, S.; Sopory, S. K.; Reddy, M. K. Identification of salt-induced genes from *Salicornia brachiata*, an extreme halophyte through expressed sequence tags analysis. *Genes Genet. Syst.* **2009**, *84* (2), 111–120.

(18) Diedhiou, C. J.; Popova, O. V.; Golldack, D. Transcript profiling of the salt-tolerant *Festuca rubra* ssp. *litoralis* reveals a regulatory network controlling salt acclimatization. *J. Plant Physiol.* **2009**, *166* (7), 697–711.

(19) Wang, X.; Fan, P.; Song, H.; Chen, X.; Li, X.; Li, Y. Comparative proteomic analysis of differentially expressed proteins in shoots of *Salicornia europaea* under different salinity. *J. Proteome Res.* **2009**, *8* (7), 3331–3345.

(20) Askari, H.; Edqvist, J.; Hajheidari, M.; Kafi, M.; Salekdeh, G. H. Effects of salinity levels on proteome of *Suaeda aegyptiaca* leaves. *Proteomics* **2006**, *6* (8), 2542–2554.

(21) Tada, Y.; Kashimura, T. Proteomic analysis of salt-responsive proteins in the mangrove plant, *Bruguiera gymnorhiza*. *Plant Cell Physiol.* **2009**, *50* (3), 439–446.

(22) Pang, Q.; Chen, S.; Dai, S.; Chen, Y.; Wang, Y.; Yan, X. Comparative proteomics of salt tolerance in *Arabidopsis thaliana* and *Thellungiella halophila*. *J. Proteome Res.* **2010**, *9* (5), 2584–2599.

(23) Sobhanian, H.; Motamed, N.; Jazii, F. R.; Nakamura, T.; Komatsu, S. Salt stress induced differential proteome and metabolome response in the shoots of *Aeluropus lagopoides* (Poaceae), a halophyte C4 plant. *J. Proteome Res.* **2010**, *9* (6), 2882–2897.

(24) Sengupta, S.; Majumder, A. L. Insight into the salt tolerance factors of a wild halophytic rice, *Porteresia coarctata*: a physiological and proteomic approach. *Planta* **2009**, *229* (4), 911–929.

(25) Geissler, N.; Hussin, S.; Koyro, H. W. Elevated atmospheric CO_2 concentration enhances salinity tolerance in *Aster tripolium* L. *Planta* **2010**, *231* (3), 583–594.

(26) Guo, L. Q.; Shi, D. C.; Wang, D. L. The key physiological response to alkali stress by the alkali-resistant halophyte *Puccinellia tenuiflora* is the accumulation of large quantities of organic acids and into the rhyzosphere. *J. Agron. Crop. Sci.* **2010**, *196* (2), 123–135.

(27) Yan, X. F.; Sun, G. R.; Li, J. Changes of several osmotica in *Puccinellia tenuiflora* seedling under alkali salt stress. *Bull. Bot. Res.* **1999**, *19* (3), 347–355.

(28) Shi, D. C.; Yin, S. J.; Yang, G. H.; Zhao, K. F. Citric acid accumulation in an alkali-tolerant plant *Puccinellia tenuiflora* under alkaline stress. *Acta Bot. Sin.* **2002**, *44* (5), 537–540.

(29) Peng, Y. H.; Zhu, Y. F.; Mao, Y. Q.; Wang, S. M.; Su, W. A.; Tang, Z. C. Alkali grass resists salt stress through high $[K^+]$ and an endodermis barrier to Na. *J. Exp. Bot.* **2004**, *55* (398), 939–949.

(30) Wang, C. M.; Zhang, J. L.; Liu, X. S.; Li, Z.; Wu, G. Q.; Cai, J. Y.; Flowers, T. J.; Wang, S. M. *Puccinellia tenuiflora* maintains a low Na^+ level under salinity by limiting unidirectional Na^+ influx resulting in a high selectivity for K^+ over Na^+. *Plant Cell Environ.* **2009**, *32* (5), 486–496.

(31) Sun, G. R.; Peng, Y. Z.; Shao, H. B.; Chu, L. Y.; Zhao, X. N.; Min, H. Y.; Cao, W. Z.; Wei, C. X. Does *Puccinelia tenuiflora* have the ability of salt exudation?. *Colloids Surf., B* **2005**, *46* (4), 197–203.

(32) Wang, Y. X.; Sun, G. R.; Suo, B.; Chen, G.; Wang, J. B.; Yan, Y. Effects of Na_2CO_3 and NaCl stresses on the antioxidant enzymes of chloroplasts and chlorophyll fluorescence parameters of leaves of *Puccinellia tenuiflora* (Turcz.) scribn.et Merr. *Acta Physiol. Plant* **2008**, *30* (2), 143–150.

(33) Zhang, C. Q.; Nishiuchi, S.; Liu, S. K.; Takano, T. Characterization of two plasma membrane protein 3 genes (*PutPMP3*) from the alkali grass, *Puccinellia tenuiflora*, and functional comparison of the rice homologues, *OsLti6a/b* from rice. *BMB Rep.* **2008**, *41* (6), 448–454.

(34) Ardie, S. W.; Xie, L.; Takahashi, R.; Liu, S.; Takano, T. Cloning of a high-affinity K^+ transporter gene *PutHKT2;1* from *Puccinellia tenuiflora* and its functional comparison with *OsHKT2;1* from rice in yeast and *Arabidopsis*. *J. Exp. Bot.* **2009**, *60* (12), 3491–3502.

(35) Ardie, S. W.; Liu, S.; Takano, T. Expression of the AKT1-type K^+ channel gene from *Puccinellia tenuiflora*, *PutAKT1*, enhances salt tolerance in *Arabidopsis*. *Plant Cell Rep.* **2010**, *29* (8), 865–874.

(36) Ardie, S. W.; Nishiuchi, S.; Liu, S.; Takano, T. Ectopic expression of the K^+ channel beta subunits from *Puccinellia tenuiflora* (*KPutB1*) and rice (*KOB1*) alters K^+ homeostasis of yeast and *Arabidopsis*. *Mol. Biotechnol.* **2011**, *48* (1), 76–86.

(37) Liu, H.; Zhang, X.; Takano, T.; Liu, S. Characterization of a *PutCAX1* gene from *Puccinellia tenuiflora* that confers Ca^{2+} and Ba^{2+} tolerance in yeast. *Biochem. Biophys. Res. Commun.* **2009**, *383* (4), 392–396.

(38) Wang, X.; Yang, R.; Wang, B.; Liu, G.; Yang, C.; Cheng, Y. Functional characterization of a plasma membrane Na^+/H^+ antiporter from alkali grass (*Puccinellia tenuiflora*). *Mol. Biol. Rep.* **2010**, Epub ahead of pring, DOI 10.1007/s11033-11010-10624-y.

(39) Wang, Y. X.; Sun, G. R.; Wang, J. B.; Cao, W. Z.; Liang, J. S.; Yu, Z. Z.; Lu, Z. H. Relationships among MDA content,plasma membrane permeability and the chlorophyll fluorescence parameters of *Puccinellia tenuiflora* seedlings under NaCl stress. *Acta Ecol. Sin.* **2006**, *26* (1), 122–129.

(40) Cao, J. G.; Bao, W. M.; Dai, S. J. Ultrastructure of the blepharoplast and the multilayered structure in spermatogenesis in *Osmunda cinnamomea* var. *asiatica*. *Acta Bot. Sin.* **2003**, *45* (7), 832–842.

(41) Ni, R. J.; Shen, Z.; Yang, C. P.; Wu, Y. D.; Bi, Y. D.; Wang, B. C. Identification of low abundance polyA-binding proteins in Arabidopsis chloroplast using polyA-affinity column. *Mol. Biol. Rep.* **2010**, *37* (2), 637–641.

(42) Wang, X.; Chen, S.; Zhang, H.; Shi, L.; Cao, F.; Guo, L.; Xie, Y.; Wang, T.; Yan, X.; Dai, S. Desiccation tolerance mechanism in resurrection fern-ally *Selaginella tamariscina* revealed by physiological and proteomic analysis. *J. Proteome Res.* **2010**, *9* (12), 6561–6577.

(43) Li, H. S.; Sun, Q.; Zhao, S. J.; Zhang, W. H. *Principles and Techniques of Plant Physiological Biochemical Experiment*; Higher Education Press: Beijing, 2000.

(44) Ma, W.; Wei, L.; Wang, Q. The response of electron transport mediated by active NADPH dehydrogenase complexes to heat stress in the *cyanobacterium Synechocystis* 6803. *Sci. China, Ser. C: Life Sci.* 2008, *51* (12), 1082–1087.

(45) Bradford, M. M. A rapid and sensitive method for the quantitation of microgram quantities of protein utilizing the principle of protein-dye binding. *Anal. Biochem.* 1976, *72* (1–2), 248–254.

(46) Ching, L. S.; Mohamed, S. Alpha-tocopherol content in 62 edible tropical plants. *J. Agric. Food Chem.* 2001, *49* (6), 3101–3105.

(47) Dai, S.; Li, L.; Chen, T.; Chong, K.; Xue, Y.; Wang, T. Proteomic analyses of *Oryza sativa* mature pollen reveal novel proteins associated with pollen germination and tube growth. *Proteomics* 2006, *6* (8), 2504–2529.

(48) Zhu, M.; Dai, S.; McClung, S.; Yan, X.; Chen, S. Functional differentiation of *Brassica napus* guard cells and mesophyll cells revealed by comparative proteomics. *Mol. Cell Proteomics* 2009, *8* (4), 752–766.

(49) Baker, N. R. Chlorophyll fluorescence: a probe of photosynthesis in vivo. *Annu. Rev. Plant Biol.* 2008, *59*, 89–113.

(50) Wang, H. L.; Lee, P. D.; Liu, L. F.; Su, J. C. Effect of sorbitol induced osmotic stress on the changes of carbohydrate and free amino acid pools in sweet potato cell suspension cultures. *Bot. Bull. Acad. Sin* 1999, *40*, 219–225.

(51) Wang, Y.; Yang, C.; Liu, G.; Jiang, J. Development of a cDNA microarray to identify gene expression of *Puccinellia tenuiflora* under saline-alkali stress. *Plant Physiol. Biochem.* 2007, *45* (8), 567–576.

(52) Ramagopal, S. Salinity stress induced tissue-specific proteins in barley seedlings. *Plant Physiol.* 1987, *84* (2), 324–331.

(53) Munoz, G. E.; Marin, K.; Gonzalez, C. Polypeptide profile in *Prosopis* seedlings growing in saline conditions. *Phyton (Buenos Aires, Argent.)* 1997, *61*, 17–24.

(54) El-Shintinawy, F.; El-Shourbagy, M. N. Alleviation of changes in protein metabolism in NaCl-stressed wheat seedlings by thiamine. *Biol. Plant.* 2001, *44* (4), 541–545.

(55) Parida, A. K.; Das, A. B.; Mittra, B.; Mohanty, P. Salt-stress induced alterations in protein profile and protease activity in the mangrove *Bruguiera parviflora*. *Z. Naturforsch. C* 2004, *59* (5−6), 408–414.

(56) Yang, C.; Chong, J.; Li, C.; Kim, C.; Shi, D.; Wang, D. Osmotic adjustment and ion balance traits of an alkali resistant halophyte *Kochia sieversiana* during adaptation to salt and alkali conditions. *Plant Soil* 2007, *294* (1), 263–276.

(57) Zhu, J. K. Regulation of ion homeostasis under salt stress. *Curr. Opin. Plant Biol.* 2003, *6* (5), 441–445.

(58) Rozema, J.; Gude, H.; Pollak, G. An ecophysiological study of the salt secretion of four halophytes. *New Phytol.* 1981, *89* (2), 201–217.

(59) Niyogi, K. K. Photoprotection revisited: Genetic and molecular approaches. *Annu. Rev. Plant Physiol. Plant Mol. Biol.* 1999, *50*, 333–359.

(60) Khan, M. A.; Ungar, I. A.; Showalter, A. M. Effects of salinity on growth, water relations and ion accumulation of the subtropical perennial halophyte, *Atriplex griffithii* var. *stocksii*. *Ann. Bot.* 2000, *85* (2), 225–232.

(61) Nemati, I.; Moradi, F.; Gholizadeh, S.; Esmaeili, M. A.; Bihamta, M. R. The effect of salinity stress on ions and soluble sugars distribution in leaves, leaf sheaths and roots of rice (*Oryza sativa* L.) seedlings. *Plant Soil Environ.* 2011, *57* (1), 26–33.

(62) Boursier, P.; Lynch, J.; Lauchli, A.; Epstein, E. Chloride partitioning in leaves of salt-stressed sorghum, maize, wheat and barley. *Funct. Plant Biol.* 1987, *14* (4), 463–473.

(63) Liu, J.; Shi, D. C. Photosynthesis, chlorophyll fluorescence, inorganic ion and organic acid accumulations of sunflower in responses to salt and salt-alkaline mixed stress. *Photosynthetica* 2010, *48* (1), 127–134.

(64) Redondo-Gomez, S.; Mateos-Naranjo, E.; Davy, A. J.; Fernandez-Munoz, F.; Castellanos, E. M.; Luque, T.; Figueroa, M. E. Growth and photosynthetic responses to salinity of the salt-marsh shrub *Atriplex portulacoides*. *Ann. Bot.* 2007, *100* (3), 555–563.

(65) Centritto, M.; Loreto, F.; Chartzoulakis, K. The use of low [CO_2] to estimate diffusional and non-diffusional limitations of photosynthetic capacity of salt-stressed olive saplings. *Plant Cell Environ.* 2003, *26* (4), 585–594.

(66) Lee, G.; Carrow, R. N.; Duncan, R. R. Photosynthetic responses to salinity stress of halophytic *Seashore paspalum* ecotypes. *Plant Sci.* 2004, *166* (6), 1417–1425.

(67) Lu, C.; Qiu, N.; Wang, B.; Zhang, J. Salinity treatment shows no effects on photosystem II photochemistry, but increases the resistance of photosystem II to heat stress in halophyte *Suaeda salsa*. *J. Exp. Bot.* 2003, *54* (383), 851–860.

(68) Jithesh, M. N.; Prashanth, S. R.; Sivaprakash, K. R.; Parida, A. K. Antioxidative response mechanisms in halophytes: their role in stress defence. *J. Genet.* 2006, *85* (3), 237–254.

(69) Moreno, J. I.; Martin, R.; Castresana, C. Arabidopsis SHMT1, a serine hydroxymethyltransferase that functions in the photorespiratory pathway influences resistance to biotic and abiotic stress. *Plant J.* 2005, *41* (3), 451–463.

(70) DellaPenna, D.; Pogson, B. J. Vitamin synthesis in plants: tocopherols and carotenoids. *Annu. Rev. Plant Biol.* 2006, *57*, 711–738.

(71) Havaux, M.; Eymery, F.; Porfirova, S.; Rey, P.; Dormann, P. Vitamin E protects against photoinhibition and photooxidative stress in *Arabidopsis thaliana*. *Plant Cell* 2005, *17* (12), 3451–3469.

(72) Munne-Bosch, S. The role of alpha-tocopherol in plant stress tolerance. *J. Plant Physiol.* 2005, *162* (7), 743–748.

(73) Miller, G.; Suzuki, N.; Ciftci-Yilmaz, S.; Mittler, R. Reactive oxygen species homeostasis and signalling during drought and salinity stresses. *Plant Cell Environ.* 2010, *33* (4), 453–467.

(74) Krapp, A. R.; Tognetti, V. B.; Carrillo, N.; Acevedo, A. The role of ferredoxin-NADP$^+$ reductase in the concerted cell defense against oxidative damage. *Eur. J. Biochem.* 1997, *249* (2), 556–563.

(75) Henkes, S.; Sonnewald, U.; Badur, R.; Flachmann, R.; Stitt, M. A small decrease of plastid transketolase activity in antisense tobacco transformants has dramatic effects on photosynthesis and phenylpropanoid metabolism. *Plant Cell* 2001, *13* (3), 535–551.

(76) Nemoto, Y.; Sasakuma, T. Specific expression of glucose-6-phosphate dehydrogenase (G6PDH) gene by salt stress in wheat (*Triticum aestivum* L.). *Plant Sci.* 2000, *158* (1−2), 53–60.

(77) Fahrendorf, T.; Ni, W.; Shorrosh, B. S.; Dixon, R. A. Stress responses in alfalfa (*Medicago sativa* L.) XIX. Transcriptional activation of oxidative pentose phosphate pathway genes at the onset of the isoflavonoid phytoalexin response. *Plant Mol. Biol.* 1995, *28* (5), 885–900.

(78) Katz, A.; Waridel, P.; Shevchenko, A.; Pick, U. Salt-induced changes in the plasma membrane proteome of the halotolerant alga *Dunaliella salina* as revealed by blue native gel electrophoresis and nano-LC-MS/MS analysis. *Mol. Cell Proteomics* 2007, *6* (9), 1459–1472.

(79) Kruger, N. J.; von Schaewen, A. The oxidative pentose phosphate pathway: structure and organisation. *Curr. Opin. Plant Biol.* 2003, *6* (3), 236–246.

(80) Ma, Q. H.; Xu, Y.; Lin, Z. B.; He, P. Cloning of cDNA encoding COMT from wheat which is differentially expressed in lodging-sensitive and -resistant cultivars. *J. Exp. Bot.* 2002, *53* (378), 2281–2282.

(81) Sanchez-Aguayo, I.; Rodriguez-Galan, J. M.; Garcia, R.; Torreblanca, J.; Pardo, J. M. Salt stress enhances xylem development and expression of S-adenosyl-L-methionine synthase in lignifying tissues of tomato plants. *Planta* 2004, *220* (2), 278–285.

(82) Hu, Y.; Li, W. C.; Xu, Y. Q.; Li, G. J.; Liao, Y.; Fu, F. L. Differential expression of candidate genes for lignin biosynthesis under drought stress in maize leaves. *J. Appl. Genet.* 2009, *50* (3), 213–223.

(83) Shen, Z.; Li, P.; Ni, R. J.; Ritchie, M.; Yang, C. P.; Liu, G. F.; Ma, W.; Liu, G. J.; Ma, L.; Li, S. J.; Wei, Z. G.; Wang, H. X.; Wang, B. C. Label-free quantitative proteomics analysis of etiolated maize seedling leaves during greening. *Mol. Cell Proteomics* 2009, *8* (11), 2443–2460.

(84) Parsley, K.; Hibberd, J. M. The Arabidopsis PPDK gene is transcribed from two promoters to produce differentially expressed

transcripts responsible for cytosolic and plastidic proteins. *Plant Mol. Biol.* **2006**, *62* (3), 339–349.

(85) Moons, A.; Valcke, R.; Van Montagu, M. Low-oxygen stress and water deficit induce cytosolic pyruvate orthophosphate dikinase (PPDK) expression in roots of rice, a C_3 plant. *Plant J.* **1998**, *15* (1), 89–98.

(86) Hibberd, J. M.; Quick, W. P. Characteristics of C4 photosynthesis in stems and petioles of C3 flowering plants. *Nature* **2002**, *415* (6870), 451–454.